Vacuum polarization energy decline and spontaneous positron emission in QED under Coulomb supercriticality

P. Grashin* and K. Sveshnikov†

Department of Physics and Institute of Theoretical Problems of Microworld, Moscow State University, 119991 Leninsky Gory, Moscow, Russia

(Received 24 January 2022; accepted 19 June 2022; published 11 July 2022)

The properties of QED-vacuum polarization, caused by the supercritical external Coulomb source with charge Z and size R, are explored in an essentially nonperturbative approach with emphasis on the vacuum energy $\mathcal{E}_{\mathrm{VP}}$ (where VP stands for vacuum polarization.) It is shown that in the supercritical region $\mathcal{E}_{\mathrm{VP}}$ turns out to be a decreasing function of the Coulomb charge, resulting in decay into the negative range as $\sim -Z^4/R$. Moreover, it is indeed the decline of $\mathcal{E}_{\mathrm{VP}}$, which provides the required energy for (presumably possible) positron emission. Found this way, properties of the resonance decay are in agreement with those achieved by other methods. The additional problems of spontaneous emission, caused by lepton number, are also discussed.

DOI: 10.1103/PhysRevD.106.013003

I. INTRODUCTION

So far, the assumption of a deep QED-vacuum reconstruction, caused by discrete levels diving into the lower continuum and accompanied by such nontrivial effects as spontaneous positron emission combined with vacuum shells formation (see, e.g., Refs. [1–5] and citations therein), is subject to active research [1,6–11]. In $3+1$ QED, such effects are expected for extended Coulomb sources of nucleus size with charges $Z > Z_{\mathrm{cr},1} \simeq 170$, which are large enough for direct observation and probably could be created in low-energy heavy-ion collisions at new heavy-ion facilities FAIR (Darmstadt), NICA (Dubna), and HIAF (Lanzhou) [12–14].

Since any process of emission must be first analyzed via energy balance in the system, in the present paper the nonperturbative vacuum polarization (VP) effects, caused by the quasistatic supercritical Coulomb sources with $Z > Z_{\mathrm{cr},1}$, are explored in terms of VP energy $\mathcal{E}_{\mathrm{VP}}$. The reason is that the spontaneous emission of positrons should be provided solely by VP effects without any other channels of energy transfer. $\mathcal{E}_{\mathrm{VP}}$ plays an essential role in the region of supercriticality. In particular, $\mathcal{E}_{\mathrm{VP}}$ being considered as a function of Z reveals with growing Z a pronounced decline into the negative range, accompanied with negative jumps, exactly equal to the electron rest mass, which occur each time the discrete level dives into the lower continuum. Moreover, it is indeed the decline of $\mathcal{E}_{\mathrm{VP}}$ that provides the spontaneous positrons with corresponding energy for emission. In turn, the emitted positrons carry away the lepton number equal to $(-1)\times$ their total number, and so the corresponding amount of positive lepton numbers must be transferred to VP density, concentrated in vacuum shells. In this case, instead of an integer lepton number of real particles there should appear the lepton number VP density. Otherwise, either the lepton number conservation in such processes must be broken or the spontaneous positron emission prohibited. In view of recent attempts in this field of interest [1,6,9–14], the last circumstance requires additional attention.

These questions are explored within the Dirac-Coulomb (DC) problem with external static or adiabatically slowly varying spherically symmetric Coulomb potential, created by a uniformly charged sphere

$$V(r) = -Z\alpha\left(\frac{1}{R(Z)}\theta(R(Z)-r) + \frac{1}{r}\theta(r-R(Z))\right) \tag{1}$$

or charged ball

$$V(r) = -Z\alpha\left(\frac{3R^2(Z)-r^2}{2R^3(Z)}\theta(R(Z)-r) + \frac{1}{r}\theta(r-R(Z))\right). \tag{2}$$

Here and henceforth,

$$Q = Z\alpha, \tag{3}$$

while the relation between the radius of the Coulomb source and its charge is given by

*grashin4@gmail.com
†k.sveshnikov@gmail.com

$$R(Z) \simeq 1.2(2.5Z)^{1/3}\ \text{fm}, \tag{4}$$

which roughly imitates the size of a superheavy nucleus with charge Z. In what follows, $R(Z)$ will be quite frequently denoted simply as R.

It should be specially noted that the parameter Q plays actually the role of the effective coupling constant for VP effects under question. The size of the source $R(Z)$ and its shape are also the additional input parameters, but their role in VP effects is quite different from Q and in some important questions, in particular, in the renormalization procedure, this difference must be clearly tracked. Furthermore, the difference between the charged sphere and the ball, which seems more preferable as a model of superheavy nucleus or heavy-ion cluster, in VP effects of Coulomb supercriticality is small. At the same time, the spherical shell model allows for an almost completely analytical study of the problem, which has clear advantages in many positions. The ball model does not share such options, since explicit solution of the DC problem in this case is absent, and so one has to use from the beginning the numerical methods or special approximations. We will briefly consider one of such approximations at the end of Sec. V and in Appendix B.

As in basic works on this topic [1–5,15–17], radiative corrections from virtual photons are neglected. Henceforth, if it is not stipulated separately, relativistic units $\hbar = m_e = c = 1$ and the standard representation of Dirac matrices are used. Concrete calculations, illustrating the general picture, are performed for $\alpha = 1/137.036$ by means of computer algebra systems (such as Maple 21) to facilitate the analytic calculations and GNU OCTAVE code for boosting the numerical work.

II. PERTURBATIVE APPROACH TO $\mathcal{E}_{\text{VP}}$

It this section, it would be pertinent to show explicitly the dependence on m. To the leading order, the perturbative VP energy $\mathcal{E}^{(1)}_{\text{VP}}$ is obtained from the general first-order Schwinger relation [4,18,19]

$$\mathcal{E}^{(1)}_{\text{VP}} = \frac{1}{2}\int d\vec{r}\varrho^{(1)}_{\text{VP}}(\vec{r})A^{\text{ext}}_0(\vec{r}), \tag{5}$$

where $\varrho^{(1)}_{\text{VP}}(\vec{r})$ is the first-order perturbative VP density, which is obtained from the one-loop (Uehling) potential $A^{(1)}_{\text{VP},0}(\vec{r})$ in the following way:

$$\varrho^{(1)}_{\text{VP}}(\vec{r}) = -\frac{1}{4\pi}\Delta A^{(1)}_{\text{VP},0}(\vec{r}), \tag{6}$$

where

$$A^{(1)}_{\text{VP},0}(\vec{r}) = \frac{1}{(2\pi)^3}\int d\vec{q}\mathrm{e}^{i\vec{q}\,\vec{r}}\Pi_R(-\vec{q}^2)\tilde{A}_0(\vec{q}),$$
$$\tilde{A}_0(\vec{q}) = \int d\vec{r}'\mathrm{e}^{-i\vec{q}\vec{r}'}A^{\text{ext}}_0(\vec{r}'). \tag{7}$$

The polarization function $\Pi_R(q^2)$, which enters Eq. (7), is defined via general relation $\Pi^{\mu\nu}_R(q) = (q^\mu q^\nu - g^{\mu\nu}q^2)\Pi_R(q^2)$ and so is dimensionless. In the adiabatic case under consideration, $q^0 = 0$ and $\Pi_R(-\vec{q}^2)$ takes the form

$$\Pi_R(-\vec{q}^2) = \frac{2\alpha}{\pi}\int_0^1 d\beta\,\beta(1-\beta)\ln\left[1+\beta(1-\beta)\frac{\vec{q}^2}{m^2 - i\epsilon}\right]$$
$$= \frac{\alpha}{\pi}S(|\vec{q}|/m), \tag{8}$$

where

$$S(x) = -5/9 + 4/3x^2 + (x^2-2)\sqrt{x^2+4}$$
$$\times \ln\left[(\sqrt{x^2+4}+x)/(\sqrt{x^2+4}-x)\right]/3x^3. \tag{9}$$

Proceeding further, from (5)–(7) one finds

$$\mathcal{E}^{(1)}_{\text{VP}} = \frac{1}{64\pi^4}\int d\vec{q}\,\vec{q}^2\Pi_R(-\vec{q}^2)\left|\int d\vec{r}\,\mathrm{e}^{i\vec{q}\,\vec{r}}A^{\text{ext}}_0(\vec{r})\right|^2. \tag{10}$$

Note that, since the function $S(x)$ is strictly positive, the perturbative VP energy is also positive, as predicted in pioneering works on QED-vacuum polarization [18].

In the spherically symmetric case with $A^{\text{ext}}_0(\vec{r}) = A_0(r)$ the perturbative VP term belongs to the s channel and equals

$$\mathcal{E}^{(1)}_{\text{VP}} = \frac{1}{\pi}\int_0^\infty dq\,q^4\Pi_R(-q^2)\left(\int_0^\infty r^2 dr j_0(qr)A_0(r)\right)^2. \tag{11}$$

By means of condition

$$mR(Z) \ll 1, \tag{12}$$

which is satisfied by the Coulomb source with relation (4) between its charge and radius up to $Z \sim 1000$, the integrals in (11) can be calculated analytically (see Ref. [3] for details). In particular,

$$\mathcal{E}^{(1)}_{\text{VP,sphere}} = \frac{Q^2}{3\pi R}\left[\ln\left(\frac{1}{2mR}\right) - \gamma_E + \frac{1}{6}\right],$$
$$\mathcal{E}^{(1)}_{\text{VP,ball}} = \frac{2Q^2}{5\pi R}\left[\ln\left(\frac{1}{2mR}\right) - \gamma_E + \frac{1}{5}\right]. \tag{13}$$

It should be remarked that if the condition (12) is satisfied, then the ratio

$$\mathcal{E}^{(1)}_{\mathrm{VP,ball}}/\mathcal{E}^{(1)}_{\mathrm{VP,sphere}} \simeq 6/5 \tag{14}$$

is the same as for their classical electrostatic self-energies $3Z^2\alpha/5R$ and $Z^2\alpha/2R$.

III. VP ENERGY IN THE NONPERTURBATIVE APPROACH

The starting expression for $\mathcal{E}_{\mathrm{VP}}$ is

$$\mathcal{E}_{\mathrm{VP}} = \frac{1}{2}\left(\sum_{\epsilon_n<\epsilon_F}\epsilon_n - \sum_{\epsilon_n\geq\epsilon_F}\epsilon_n\right), \tag{15}$$

where $\epsilon_F = -1$ is the Fermi level, which in such problems with strong Coulomb fields is chosen at the lower threshold, while ϵ_n are the eigenvalues of the corresponding DC problem.

Expression (15) is obtained from the Dirac Hamiltonian, written in the form that is consistent with Schwinger prescription for the current (for details see, e.g., Ref. [3]) and is defined up to a constant, depending on the choice of the energy reference point. Actually, $\mathcal{E}_{\mathrm{VP}}$ is nothing else but the Casimir vacuum energy for the electron-positron system [3]. Following the general prescription for Casimir energy calculations [3,19], the natural choice of the reference point for $\mathcal{E}_{\mathrm{VP}}$ is the free case $A_{\mathrm{ext}} = 0$. In the present case, the latter must be combined with the circumstance that, unlike the purely photonic Casimir effect, there exists also an infinite set of discrete Coulomb levels. To pick out exclusively the interaction effects, it is therefore necessary to subtract in addition from each discrete level the mass of the free electron at rest.

Thus, in the physically motivated form and in agreement with the VP density ϱ_{VP}, which is defined so that it automatically vanishes in the free case [3,4,15,16,18], the initial expression for the VP energy should be written as

$$\mathcal{E}_{\mathrm{VP}} = \frac{1}{2}\left(\sum_{\epsilon_n<\epsilon_F}\epsilon_n - \sum_{\epsilon_n\geq\epsilon_F}\epsilon_n + \sum_{-1\leq\epsilon_n<1} 1\right)_A - \frac{1}{2}\left(\sum_{\epsilon_n\leq -1}\epsilon_n - \sum_{\epsilon_n\geq 1}\epsilon_n\right)_0, \tag{16}$$

where the label A denotes the nonvanishing external field A_{ext}, while the label 0 corresponds to $A_{\mathrm{ext}} = 0$. Defined in such a way, VP energy vanishes by turning off the external field, while by turning it on, it contains only the interaction effects, and so the expansion of $\mathcal{E}_{\mathrm{VP}}$ in (even) powers of the external field starts from $O(Q^2)$.

For what follows, it would be pertinent to introduce a number of additional definitions and notations. The reason is that the purely Coulomb problem with spherical symmetry is just a start-up for more complicated problems, where only the axial symmetry is preserved. These are, in particular, the two-center Coulomb one, which imitates the slow collision of two heavy ions, and the one-center Coulomb one in the presence of an axial magnetic field. In such problems, the total angular moment $\vec{j}$ is not conserved; there remains only its projection m_j. As a consequence, the angular quantum number $k = \pm(j+1/2)$, which is very suitable for enumerating the Coulomb states of the Dirac fermion both in momentum and parity, becomes out of work. In this situation, it is useful to represent the Dirac bispinor with fixed m_j in the form

$$\psi_{m_j}(\vec{r}) = \begin{pmatrix} \varphi_{m_j}(\vec{r}) \\ -i\chi_{m_j}(\vec{r}) \end{pmatrix}, \tag{17}$$

where the spinors ψ and χ are defined as the partial series over integer orbital momentum l,

$$\begin{aligned} \varphi_{m_j}(\vec{r}) &= \sum_{l=0}^{\infty}\left(u_l(r)\Omega^{(+)}_{lm_j}(\vec{n}) + v_l(r)\Omega^{(-)}_{l+1,m_j}(\vec{n})\right), \\ \chi_{m_j}(\vec{r}) &= \sum_{l=0}^{\infty}\left(p_l(r)\Omega^{(+)}_{lm_j}(\vec{n}) + q_l(r)\Omega^{(-)}_{l+1,m_j}(\vec{n})\right), \end{aligned} \tag{18}$$

with $\vec{n} = \vec{r}/r$ and $\Omega^{(\pm)}_{lm_j}(\vec{n})$ being the spherical spinors with the total momentum $j = l \pm 1/2$ and fixed $j_z = m_j$. Each term in parentheses in series (18) corresponds to $j = l + 1/2$, while from the structure of the DC problem there follows that the radial functions $u_l(r)$, $v_l(r)$, $p_l(r)$, and $q_l(r)$ can be always chosen real.

The spherical spinors are defined as follows:

$$\begin{aligned} \Omega^{(+)}_{lm_j}(\vec{n}) &= \begin{pmatrix} \sqrt{\frac{l+m_j+1/2}{2l+1}}Y_{l,m_j-1/2} \\ \sqrt{\frac{l-m_j+1/2}{2l+1}}Y_{l,m_j+1/2} \end{pmatrix}, \\ \Omega^{(-)}_{lm_j}(\vec{n}) &= \begin{pmatrix} \sqrt{\frac{l-m_j+1/2}{2l+1}}Y_{l,m_j-1/2} \\ -\sqrt{\frac{l+m_j+1/2}{2l+1}}Y_{l,m_j+1/2} \end{pmatrix}, \end{aligned} \tag{19}$$

whence $(\vec{\sigma}\,\vec{n})\Omega^{(+)}_{lm_j}(\vec{n}) = \Omega^{(-)}_{l+1,m_j}(\vec{n})$, whereas the phase of spherical functions is chosen in a standard way, providing $l_\pm Y_{lm} = \sqrt{(l\mp m)(l\pm m+1)}Y_{l,m\pm1}$ and $Y_{l,-|m|} = (-1)^{|m|}Y^*_{l,|m|}$.

For the spherically symmetric Coulomb potential $V(r)$ of the type (1) and (2), the spectral DC problem for the energy level ϵ divides into two radial subsystems, containing either (u_l, q_l) or (p_l, v_l) pairs, of the following form:

$$\begin{cases} \left(\partial_r - \frac{l}{r}\right) u_l = (\epsilon - V(r) + 1) q_l, \\ \left(\partial_r + \frac{l+2}{r}\right) q_l = -(\epsilon - V(r) - 1) u_l, \end{cases} \tag{20}$$

$$\begin{cases} \left(\partial_r - \frac{l}{r}\right) p_l = -(\epsilon - V(r) - 1) v_l, \\ \left(\partial_r + \frac{l+2}{r}\right) v_l = (\epsilon - V(r) + 1) p_l. \end{cases} \tag{21}$$

Equations (20) and (21) are subject of crossing symmetry: under simultaneous change of the sign of external potential and energy $Q \to -Q$ and $\epsilon \to -\epsilon$, the pairs (u_l, q_l) and (p_l, v_l) interchange. This symmetry will be used further by calculation of the VP energy via the phase integral method.

Now let us extract from (16) separately the contributions from the discrete and continuous spectra for each value of orbital momentum l, and afterward use for the difference of integrals over continua $(\int d\vec{k}\sqrt{k^2+1})_A - (\int d\vec{k}\sqrt{k^2+1})_0$ the well-known technique, which represents this difference in the form of an integral of the elastic scattering phase $\delta_l(k)$ [8,20–22]. Compared to the one-dimensional case considered in detail in Ref. [8], the only difference is that instead of the one-dimensional bag $-L \le x \le +L$ with boundary condition $i\alpha\psi(\pm L) \pm \beta\psi(\pm L) = 0$ in the present case, one has to use the three-dimensional fermionic bag confinement condition [23]

$$(i\vec{n}\,\vec{\alpha} + \beta)\psi|_{R_{\rm bag}} = 0. \tag{22}$$

Within the partial expansion (17) and (18), the boundary condition (22) transforms into

$$(u_l + q_l)|_{R_{\rm bag}} = (p_l + v_l)|_{R_{\rm bag}} = 0. \tag{23}$$

Further steps for each partial term repeat completely those of Ref. [8] and yield the final answer for $\mathcal{E}_{\rm VP}(Z)$, which as a partial series over angular momentum l is given by the following expression:

$$\mathcal{E}_{\rm VP}(Z) = \sum_{l=0} \mathcal{E}_{{\rm VP},l}(Z), \tag{24}$$

where

$$\mathcal{E}_{{\rm VP},l}(Z) = (l+1)\left(\frac{1}{\pi}\int_0^\infty \frac{kdk}{\sqrt{k^2+1}}\delta_{\rm tot}(l,k) + \sum_{\pm}\sum_{-1\le\epsilon^{\pm}_{n,l}<1}(1-\epsilon^{\pm}_{n,l})\right). \tag{25}$$

In (25), $\delta_{\rm tot}(l,k)$ is the total phase shift for the given values of the wave number k and orbital momentum l, including the contributions of the scattering states of the problems (20) and (21) from both continua and both parities. In the discrete spectrum contribution to $\mathcal{E}_{{\rm VP},l}(Z)$, the additional sum $\sum_{\pm}$ also takes into account both parities. Note also that the multiplier $l+1$ in (25) appears as a product of the degeneracy factor $2(l+1) = 2j+1$ and $1/2$ in (16).

Such approach to evaluation of $\mathcal{E}_{\rm VP}$ turns out to be quite effective, since for the external potentials of the type (1) and (2) each partial VP energy turns out to be finite without any special regularization. First, $\delta_{\rm tot}(l,k)$ behaves both in IR and UV limits in the k variable much better than each of the scattering phase shifts separately. Namely, $\delta_{\rm tot}(l,k)$ is finite for $k \to 0$ and behaves like $O(1/k^3)$ for $k \to \infty$; hence, the phase integral in (25) is always convergent. Moreover, $\delta_{\rm tot}(l,k)$ is by construction an even function of the external field, more precisely, of the effective coupling constant Q. Thereby the complete dependence on Z is more diverse, since the latter defines also the shape of the external source and potential in a different way via (4). Second, in the bound states contribution to $\mathcal{E}_{{\rm VP},l}(Z)$, the condensation point $\epsilon^{\pm}_{n,l} \to 1$ turns out to be a regular one for each l and parity, because $1 - \epsilon^{\pm}_{n,l} \sim O(1/n^2)$ for $n \to \infty$. The latter circumstance permits one to avoid intermediate cutoff of the Coulomb asymptotics of the external potential for $r \to \infty$, which significantly simplifies all the subsequent calculations.

The principal problem of convergence of the partial series (24) can be explored along the lines of Ref. [24], which deals with the similar expansion for $\mathcal{E}_{\rm VP}(Z)$ in $2+1$ dimensions. Let us consider first the behavior of partial VP energy (25) for large $l \gg Q$. More precisely, the last condition implies

$$(l+1)^2 \gg Q^2 + 2QR. \tag{26}$$

For such l the main component $\sim Q^2$ of the total scattering phase $\delta_{\rm tot}(l,k)$ per each parity [or, equivalently, for pairs (u_l, q_l) or (p_l, v_l)] can be reliably estimated via the quasiclassical (WKB) approximation

$$\delta_{\rm WKB}(l,k) = \delta_+(l,k) + \delta_-(l,k) - 2\delta_0(l,k), \tag{27}$$

where

$$\delta_\pm(l,k) = \int dr \sqrt{(\epsilon(k) \mp V(r))^2 - 1 - \frac{(l+1)^2}{r^2}},$$
$$\delta_0(l,k) = \int dr \sqrt{k^2 - \frac{(l+1)^2}{r^2}}, \tag{28}$$

and

$$\epsilon(k) = \sqrt{k^2+1}, \tag{29}$$

while the integration is performed over regions, where the expressions under square root are non-negative. In turn, the

total WKB phase shift is twice the contribution of each parity

$$\delta_{\rm tot}^{\rm WKB}(l,k) = 2\delta_{\rm WKB}(l,k). \tag{30}$$

For a rigorous justification of such formulas for WKB phase shifts in the Dirac equation (DE) with spherically symmetric Coulomb-like potentials, see Refs. [25] (and references therein).

For the case of a charged sphere (1), all the calculations can be performed analytically and lead to the following result:

$$\begin{aligned}\delta_{\rm WKB}(l,k) = {}& \theta(0 \le k \le k_-)\pi(l+1-\varkappa_l) + \theta(k_- \le k \le k_+)\left[\pi(l+1) - \frac{\pi\varkappa_l}{2} - (l+1)\,\mathrm{arctg}\left(\frac{A_+(k)}{l+1}\right)\right.\\ & \left. + \varkappa_l\,\mathrm{arctg}\left(\frac{\epsilon(k)QR-\varkappa_l^2}{\varkappa_l A_+(k)}\right) + \frac{\epsilon(k)Q}{k}\ln\left(\frac{\sqrt{Q^2+k^2(l+1)^2}}{kA_+(k)+k^2R+\epsilon(k)Q}\right)\right]\\ & + \theta(k_+ \le k \le \infty)\left[(l+1)\left(\pi - \mathrm{arctg}\left(\frac{A_+(k)}{l+1}\right) - \mathrm{arctg}\left(\frac{A_-(k)}{l+1}\right)\right)\right.\\ & \left. + \varkappa_l\left(\mathrm{arctg}\left(\frac{\epsilon(k)QR-\varkappa_l^2}{\varkappa_l A_+(k)}\right) - \mathrm{arctg}\left(\frac{\epsilon(k)QR+\varkappa_l^2}{\varkappa_l A_-(k)}\right)\right) + \frac{\epsilon(k)Q}{k}\ln\left(\frac{kA_-(k)+k^2R-\epsilon(k)Q}{kA_+(k)+k^2R+\epsilon(k)Q}\right)\right],\end{aligned} \tag{31}$$

where

$$\varkappa_l = \sqrt{(l+1)^2 - Q^2}, \tag{32}$$

$$k_\pm = \frac{1}{R}\sqrt{(l+1)^2 + Q^2 \pm 2Q\sqrt{(l+1)^2+R^2}}, \tag{33}$$

and

$$A_\pm(k) = \sqrt{(kR)^2 \pm 2\epsilon(k)QR + Q^2 - (l+1)^2}. \tag{34}$$

The typical behavior of $\delta_{\rm WKB}(l,k)$ is shown for $Z = 100$ and $l = 100$ in Fig. 1.

The main properties of the total WKB phase (30) are the following. For $k < k_- < (l+1)/R$, it is a constant

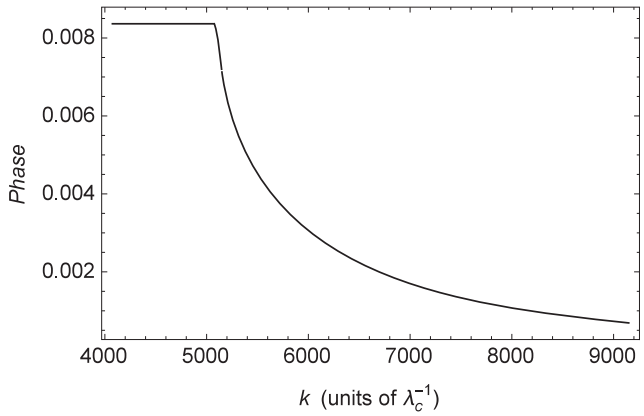

FIG. 1. $\delta_{\rm WKB}(l,k)$ for $Z = 100$ and $l = 100$.

$$\delta_{\rm tot}^{\rm WKB}(l,k) = 2\pi(l+1-\varkappa_l), \quad k < k_- < (l+1)/R, \tag{35}$$

while for large $k \gg k_+ > (l+1)/R$ it vanishes $\sim 1/k^3$, namely,

$$\delta_{\rm tot}^{\rm WKB}(l,k) \to \frac{4Q^2((l+1)^2-3R^2)}{3(kR)^3}, \quad k \gg k_+ > (l+1)/R. \tag{36}$$

In the region between k_- and k_+, it behaves as a smooth interpolation function. Moreover, the smaller the R, the greater the value of k is needed (the correct condition reads $kR \gg l$) to alter the behavior of $\delta_{\rm tot}^{\rm WKB}(l,k)$ from the constant value (35) into the decreasing one (36).

These results reproduce quite well the behavior of the exact total phase $\delta_{\rm tot}(l,k)$ with the following remarks. First, the decrease as either $O(1/k^3)$ or $O(1/y^3)$ of the uv asymptotics is a common feature of the integrands in VP integral expressions, regardless of which VP observable is under consideration. This applies equally to calculating the VP energy by means of (25) within the phase integral method or as elaborated recently in Refs. [26,27], an even more sophisticated approach to evaluate the VP energy, based on the ln[Wronskian] techniques. Second, the quasiclassical approximation does not reproduce oscillations of the exact phase for large k, which are caused by diffraction on a sphere of the radius R. In more detail, this topic is discussed within the $2+1$-dimensional case in Ref. [24].

At the same time, the behavior of both $\delta_{\rm tot}^{\rm WKB}(l,k)$ and $\delta_{\rm tot}(l,k)$ for $kR \ll l$ can be easily understood by comparing them with the total phase for a pointlike Coulomb source with the potential $V(r) = -Q/r$ (for $l+1 > Q$). The

analytic solution of the corresponding DE is well known (see, e.g., Ref. [28]) and gives the following exact answer for each of the partial phase shifts. Namely, for the (u_l, q_l) pair,

$$\delta^{\pm}_{uq}(l,k) = \frac{\pi}{2}(l+1) \pm \frac{\epsilon(k)Q}{k}\ln 2kr - \frac{\pi\varkappa_l}{2} \mp \mathrm{Arg}[\Gamma(1+\varkappa_l + i\epsilon(k)Q/k)] + \frac{1}{2}\mathrm{Arg}\left[\frac{l+1+iQ/k}{\varkappa_l \mp i\epsilon(k)Q/k}\right], \tag{37}$$

where the signs $\pm$ correspond to the phase shifts for the upper and lower continua, while for the (p_l, v_l) pair the phase shifts are obtained from (37) via simple replacement of $l+1+iQ/k \to l+1-iQ/k$ in the last term. From these results, one obtains that for all $0 \le k \le \infty$ the exact total phase for a pointlike source equals a constant

$$\delta_{\mathrm{tot}}(l,k)|_{R\to 0} = 2\pi(l+1-\varkappa_l), \tag{38}$$

which exactly coincides with the answer of the WKB approximation (35) for $k < k_- < (l+1)/R$. This result should be quite clear, since for large l the condition $kR \ll l$ implies scattering with a large impact parameter $d \gg R$. In the last case, the difference between the sphere of size R and a pointlike source is negligibly small. It should be remarked, however, that for such behavior of the exact phase the WKB condition $l \gg Q$ is crucial; otherwise, $\delta_{\mathrm{tot}}(l,k)$ for $k \to 0$ remains finite, but its limiting value in this case can be sufficiently different from (38), especially in the case $l+1 < Q$, when $\varkappa_l$ becomes imaginary [see below Eqs. (87) and (89)].

In the next step, let us consider the behavior of the partial phase integrals in (25),

$$I(l) = \frac{1}{\pi}\int_0^\infty \frac{kdk}{\sqrt{k^2+1}}\delta_{\mathrm{tot}}(l,k) \tag{39}$$

for $l \gg Q$, or more precisely, subject to condition (26). The details of this calculation are presented in Appendix A. The final result reads

$$I(l) \to \frac{2}{\pi}\int_0^\infty dr\, V^2(r) - \frac{Q^2}{l+1} + O\left(\frac{Q^4}{(l+1)^3}\right), \quad l \to \infty. \tag{40}$$

At the same time, the discrete spectrum with the same conditions on l [that means $l \to \infty$ or at least l subject to condition (26)] corresponds with high precision to the well-known solution of the Coulomb-Schrödinger problem for a pointlike source with the same Z. In this limit, the main contribution to the total sum of discrete levels comes from the vicinity of condensation point $\epsilon_{n,l} \to 1$, where both parities reveal the same properties and so can be freely treated at the same footing. The leading $\sim Q^2$ terms in bound energies of discrete levels per each parity are given by the Bohr formula

$$1 - \epsilon^{\pm}_{n_r,l} = \frac{Q^2}{2(n_r+l+1)^2}, \quad l \to \infty. \tag{41}$$

Upon summing the bound energies (41) over n_r one obtains

$$\sum_{n_r=0}^{\infty}(1-\epsilon^{\pm}_{n_r,l}) = \frac{Q^2}{2}\mathrm{Polygamma}[1,l+1] = \frac{Q^2}{2}\left(\frac{1}{(l+1)} + \frac{1}{2(l+1)^2} + \frac{1}{6(l+1)^3} + O\left(\frac{1}{(l+1)^4}\right)\right). \tag{42}$$

The next-to-leading $\sim Q^4$ terms in bound energies in this limit are given by the first relativistic (fine-structure) correction to (41),

$$Q^4\left(\frac{1}{2(l+1)(n_r+l+1)^3} - \frac{3}{8(n_r+l+1)^4}\right) \tag{43}$$

and upon summing over n_r yield the terms $\sim Q^4/(l+1)^3$ in the sum over discrete levels in $\mathcal{E}_{\mathrm{VP},l}(Z)$. At the same time, the correction to Bohr levels (41), caused by the nonvanishing size of the Coulomb source, equals [for the external potential (1)]

$$-\frac{Q^2}{(n_r+l+1)^2}\left(\frac{2QR}{n_r+l+1}\right)^{2l+2} \times \frac{(n_r+2l+1)!}{n_r!}\frac{(2l+2)(2l+3)}{(2l+3)!^2}, \tag{44}$$

and for growing l turns out to be negligibly (in fact exponentially) small, since in this limit the dominating factor in (44) is $1/(2l+3)!^2$. However, for small or even moderate l, and especially for the case $l+1 < Q$, the nonzero size of the Coulomb source plays an essential role in all the VP effects under consideration.

As a result, the partial VP energy (25) in the large l limit can be represented as

$$\mathcal{E}_{\mathrm{VP},l}(Z) = (l+1)\left[\frac{2}{\pi}\int_0^\infty dr\, V^2(r) - \frac{Q^2}{l+1} + Q^2\mathrm{Polygamma}[1,l+1] + O\left(\frac{Q^4}{(l+1)^3}\right)\right]. \tag{45}$$

Thus, in agreement with similar results in $1+1$ and $2+1$ dimensions [7,8,24,29,30], the partial series (24) for $\mathcal{E}_{\mathrm{VP}}$ diverges quadratically in the leading $O(Q^2)$ order and so

requires regularization and subsequent renormalization, although each partial $\mathcal{E}_{\mathrm{VP},l}(Z)$ in itself is finite without any additional manipulations. The degree of divergence of the partial series (24) is formally the same as in $3+1$ QED for the fermionic loop with two external lines. The latter circumstance shows that by calculation of $\mathcal{E}_{\mathrm{VP}}$ via a principally different nonperturbative approach, which does not reveal any connection with perturbation theory (PT) and Feynman graphs, we nevertheless meet the same divergence of the theory, as in PT. Actually, it should be indeed so, since both approaches deal with the same physical phenomenon (VP effects caused by the strong Coulomb field) with the main difference in the methods of calculation. Therefore, in the present approach, the cancellation of divergent terms should follow the same rules as in PT, based on regularization of the fermionic loop with two external lines, which preserves the physical content of the whole renormalization procedure and simultaneously provides the mutual agreement between perturbative and nonperturbative approaches to the calculation of $\mathcal{E}_{\mathrm{VP}}$. This conclusion is in complete agreement with results obtained earlier in Refs. [16,31].

One more but quite general reason is that for $Q \to 0$, but with fixed $R(Z)$, both the total renormalized VP density and VP energy should coincide with results obtained within PT by means of (5)–(7). Because of spherical symmetry of the external field, they both belong to the partial s channel with $l=0$. However, in the general case, the nonrenormalized (but already finite) partial VP density $\varrho_{\mathrm{VP},0}(r)$ and VP energy $\mathcal{E}_{\mathrm{VP},0}$ do not reproduce the corresponding perturbative answers for $Q \to 0$. For $\mathcal{E}^{(1)}_{\mathrm{VP}}$ and $\mathcal{E}_{\mathrm{VP},0}$, the difference is quite transparent, since the perturbative VP energy originates from the distorted continuum and so has nothing to do with the discrete levels. To the contrary, $\mathcal{E}_{\mathrm{VP},0}$ contains by construction a nonvanishing $O(Q^2)$ contribution from the latter, since for Coulomb-like potentials the discrete spectrum exists for any infinitesimally small Q.

Thus, in complete analogy with the renormalization of VP density [7,8,16,24,29–31], we should pass to the renormalized VP energy by means of relations

$$\mathcal{E}^{\mathrm{ren}}_{\mathrm{VP}}(Z) = \sum_{l=0} \mathcal{E}^{\mathrm{ren}}_{\mathrm{VP},l}(Z), \tag{46}$$

where

$$\mathcal{E}^{\mathrm{ren}}_{\mathrm{VP},l}(Z) = \mathcal{E}_{\mathrm{VP},l}(Z) + \zeta_l Z^2, \tag{47}$$

with the renormalization coefficients ζ_l defined in the following way:

$$\zeta_l = \lim_{Z_0 \to 0} \left[\frac{\mathcal{E}^{(1)}_{\mathrm{VP}}(Z_0)\delta_{l,0} - \mathcal{E}_{\mathrm{VP},l}(Z_0)}{Z_0^2} \right]_{R=R(Z)}. \tag{48}$$

The essence of relations (46)–(48) is to remove [for fixed Z and $R(Z)$!] the divergent $O(Q^2)$ component from the nonrenormalized partial terms $\mathcal{E}_{\mathrm{VP},l}(Z)$ in the series (24) and replace them further by renormalized via the fermionic loop perturbative contribution to VP energy $\mathcal{E}^{(1)}_{\mathrm{VP}}\delta_{l,0}$. Such procedure provides simultaneously the convergence of the regulated this way partial series (46) and the correct limit of $\mathcal{E}^{\mathrm{ren}}_{\mathrm{VP}}(Z)$ for $Q \to 0$ with fixed $R(Z)$.

So renormalization via fermionic loop turns out to be a universal method, which removes the divergencies of the theory simultaneously in purely perturbative and essentially nonperturbative approaches to VP. The concrete implementation of this general method depends on the VP quantity under consideration. Within the considered approach, the subtraction proceeds directly on the level of $\mathcal{E}_{\mathrm{VP},l}(Z)$ by means of (47) and (48), while the renormalization coefficients ζ_l are determined through the limiting procedure, in which the effective coupling constant $Q_0 = Z_0\alpha$ tends to zero, but the shape of the external field is preserved. So ζ_l contain a nontrivial dependence on $R(Z)$ and hence on the current charge Z of the Coulomb source. This dependence, however, has nothing to do with the renormalization procedure presented above, since the latter deals with the coupling constant $Q = Z\alpha$, but not with the shape of the external potential.

Moreover, the complete analogy between renormalizations of VP density and VP energy implies the validity of the Schwinger relation [3,4,8] for renormalized quantities

$$\delta\mathcal{E}^{\mathrm{ren}}_{\mathrm{VP}} = \int \mathrm{d}\vec{r}\varrho^{\mathrm{ren}}_{\mathrm{VP}}(\vec{r})\delta A^{\mathrm{ext}}_0(\vec{r}) + \delta\mathcal{E}_N, \tag{49}$$

since $\mathcal{E}_N$ is responsible only for jumps in the VP energy caused by discrete levels crossing through the border of the lower continuum and so is an essentially nonperturbative quantity, which does not need any renormalization. The relation (49) can be represented also in the partial form

$$\delta\mathcal{E}^{\mathrm{ren}}_{\mathrm{VP},l} = \int_0^\infty r^2 dr\, \varrho^{\mathrm{ren}}_{\mathrm{VP},l}(r)\delta A^{\mathrm{ext}}_0(r) + \delta\mathcal{E}_{N,l}, \tag{50}$$

from which it follows that the convergence of the partial series for VP density implies the convergence of the partial series for VP energy and vice versa. $\mathcal{E}_{N,l}$ is always finite and, moreover, vanishes for $l > l_{\max}(Z)$ together with discrete levels diving and therefore does not influence the convergence of the partial series.

IV. TOTAL PHASE AND DISCRETE SPECTRUM FOR THE POTENTIAL (1)

Now—having dealt with the first principles of essentially nonperturbative evaluation of VP energy by means of the phase integral method this way—let us turn to the explicit evaluation of $\mathcal{E}^{\mathrm{ren}}_{\mathrm{VP}}(Z)$ for the external potential (1). It would be pertinent to present the details of this procedure in terms of separate pairs (u_l, q_l) and (p_l, v_l), introduced via general expansion (18). Although each pair contains states with

different parity, a more detailed description of solutions of the DC problem per each parity is here of no use, since the calculation of $\mathcal{E}^{\rm ren}_{\rm VP}(Z)$ itself implies the summation over both parities.

The evaluation of total elastic phase $\delta_{\rm tot}(l,k)$ proceeds as follows. It suffices to consider only the (u_l, q_l) pair, since the contribution of the (p_l, v_l) pair to $\delta_{\rm tot}(l,k)$ can be achieved via crossing symmetry of the initial DC problem (20) and (21). First we consider the region $l+1 > Q$; that means for real $\varkappa_l$ defined in (32). In this case, in the upper continuum with

$$\epsilon(k) = +\sqrt{k^2+1} \geq 1, \tag{51}$$

the solutions of the DC problem up to a common normalization factor can be represented in the next form.

For $r \leq R(Z)$,

$$\begin{cases} u_l(k,r) = \sqrt{\epsilon(k)+V_0+1}J_{l+1/2}(\xi(k)r)/\sqrt{r}, \\ q_l(k,r) = -\sqrt{\epsilon(k)+V_0-1}J_{l+3/2}(\xi(k)r)/\sqrt{r}, \end{cases} \tag{52}$$

with $J_\nu(z)$ being the Bessel functions,

$$\xi(k) = \sqrt{(\epsilon(k)+V_0)^2-1}, \qquad V_0 = Q/R. \tag{53}$$

For $r \geq R(Z)$ the scattering states of the DC problem should be written in terms of the Kummer $\Phi(b,c,z)$ and Tricomi $\Psi(b,c,z)$ or modified Kummer $\tilde{\Phi}(b,c,z) = z^{1-c}\Phi(b-c+1, 2-c, z)$ functions [32]. The reason is that due to the Kummer relation $\Phi(b,c,x) = e^x\Phi(c-b, c, -x)$ for real $\varkappa_l$ such solutions cannot be represented in terms of $\Phi(b,c,z)$ and $\Phi^*(b,c,z)$. For our purposes, the modified Kummer function $\tilde{\Phi}(b,c,z)$ is more preferable than the Tricomi one due to the reasons of numerical calculations.

The parameters b and c of the Kummer functions are defined as

$$b_l = \varkappa_l - i\epsilon(k)Q/k, \qquad c_l = 1+2\varkappa_l. \tag{54}$$

Upon introducing the subsidiary phases ξ_1 and ξ_2,

$$\mathrm{e}^{-2i\xi_1} = \frac{b_l}{l+1+iQ/k}, \qquad \mathrm{e}^{2i\xi_2} = \frac{b_l}{l+1-iQ/k}, \tag{55}$$

and corresponding functions

$$\begin{aligned} \Phi_1(l,k,r) &= \mathrm{e}^{i(kr+\xi_1)}\Phi(b_l, c_l, -2ikr), \\ \Phi_2(l,k,r) &= \mathrm{e}^{i(kr+\xi_2-\pi\varkappa_l)}\tilde{\Phi}(b_l, c_l, -2ikr), \end{aligned} \tag{56}$$

the real-valued scattering solutions in the upper continuum are defined as follows:

$$\begin{cases} u_l(k,r) = \sqrt{\epsilon(k)+1}r^{\varkappa_l-1}(\mathrm{Re}[\Phi_1(l,k,r)] + \lambda^+_{uq}(l,k)\mathrm{Im}[\Phi_2(l,k,r)]), \\ q_l(k,r) = \sqrt{\epsilon(k)-1}r^{\varkappa_l-1}(-\mathrm{Im}[\Phi_1(l,k,r)] + \lambda^+_{uq}(l,k)\mathrm{Re}[\Phi_2(l,k,r)]), \end{cases} \tag{57}$$

with $\lambda^+_{uq}(l,k)$ being the matching coefficient between inner $r \leq R(Z)$ and outer $r \geq R(Z)$ solutions

$$\lambda^+_{uq}(l,k) = \frac{\sqrt{(\epsilon-1)(\epsilon+V_0+1)}J_{l+1/2}(\xi R)\mathrm{Im}[\Phi_1] - \sqrt{(\epsilon+1)(\epsilon+V_0-1)}J_{l+3/2}(\xi R)\mathrm{Re}[\Phi_2]}{\sqrt{(\epsilon-1)(\epsilon+V_0+1)}J_{l+1/2}(\xi R)\mathrm{Re}[\Phi_2] + \sqrt{(\epsilon+1)(\epsilon+V_0-1)}J_{l+3/2}(\xi R)\mathrm{Im}[\Phi_2]}. \tag{58}$$

On the rhs of (58), $\epsilon \equiv \epsilon(k) = +\sqrt{k^2+1} \geq 1, \xi = \xi(k)$, $R = R(Z)$, while the arguments of functions Φ_1 and Φ_2 are $(l,k,R(Z))$.

The phase shift $\delta^+_{uq}(l,k)$ in the upper continuum is defined in the standard way via asymptotics for $r \to \infty$ and equals

$$\delta^+_{uq}(l,k) = \frac{\pi l}{2} + \frac{\epsilon(k)Q}{k}\ln(2kr) + \tilde{\delta}^+_{uq}(l,k), \tag{59}$$

where

$$\tilde{\delta}^+_{uq}(l,k) = -\frac{\mathrm{Re}[A(l,k)] - \lambda^+_{uq}(l,k)\mathrm{Im}[B(l,k)]}{\mathrm{Im}[A(l,k)] + \lambda^+_{uq}(l,k)\mathrm{Re}[B(l,k)]}, \tag{60}$$

while the functions $A(l,k)$ and $B(l,k)$ are defined as follows:

$$\begin{aligned} A(l,k) &= \mathrm{e}^{-i\pi\varkappa_l/2}\frac{\Gamma(1+2\varkappa_l)}{\Gamma(\varkappa_l+i\epsilon(k)Q/k)}\sqrt{\frac{l+1+iQ/k}{\varkappa_l+i\epsilon(k)Q/k}}, \\ B(l,k) &= \mathrm{e}^{i\pi\varkappa_l/2}\frac{\Gamma(1-2\varkappa_l)}{\Gamma(-\varkappa_l+i\epsilon(k)Q/k)}\sqrt{\frac{l+1+iQ/k}{\varkappa_l-i\epsilon(k)Q/k}}. \end{aligned} \tag{61}$$

In the lower continuum, where

$$\epsilon(k) = -\sqrt{k^2+1} < -1, \tag{62}$$

the solutions are more diverse, since now the whole half-axis $0 \le k \le \infty$ should be divided in three intervals $0 \le k \le k_1$, $k_1 \le k \le k_2$, and $k_2 \le k \le \infty$, where

$$k_1 = \sqrt{(V_0 - 1)^2 - 1}, \qquad k_2 = \sqrt{(V_0 + 1)^2 - 1}. \tag{63}$$

Note that in the case under consideration V_0 turns out to be about several dozens or even hundreds, so k_1 is always well defined.

According to this division, the inner solutions of the DC problem in the lower continuum are defined as follows. For $0 \le k \le k_1$,

$$\begin{cases} u_l(k,r) = \sqrt{\epsilon(k) + V_0 + 1} J_{l+1/2}(\xi(k) r)/\sqrt{r}, \\ q_l(k,r) = -\sqrt{\epsilon(k) + V_0 - 1} J_{l+3/2}(\xi(k) r)/\sqrt{r}, \end{cases} \tag{64}$$

where $\xi(k)$ is defined as before in (53), while for the second interval $k_1 \le k \le k_2$,

$$\begin{cases} u_l(k,r) = \sqrt{\epsilon(k) + V_0 + 1} I_{l+1/2}(\tilde{\xi}(k) r)/\sqrt{r}, \\ q_l(k,r) = \sqrt{|\epsilon(k)| - V_0 + 1} I_{l+3/2}(\tilde{\xi}(k) r)/\sqrt{r}, \end{cases} \tag{65}$$

with $I_\nu(z)$ being the Infeld functions and

$$\tilde{\xi}(k) = \sqrt{1 - (\epsilon(k) + V_0)^2}. \tag{66}$$

In the third interval $k_2 \le k \le \infty$,

$$\begin{cases} u_l(k,r) = \sqrt{|\epsilon(k)| - V_0 - 1} J_{l+1/2}(\xi(k) r)/\sqrt{r}, \\ q_l(k,r) = \sqrt{|\epsilon(k)| - V_0 + 1} J_{l+3/2}(\xi(k) r)/\sqrt{r}. \end{cases} \tag{67}$$

The real-valued scattering solutions in the lower continuum are

$$\begin{cases} u_l(k,r) = \sqrt{|\epsilon(k)| - 1} r^{\varkappa_l - 1} (\mathrm{Re}[\Phi_1(l,k,r)] + \lambda^-_{uq}(l,k) \mathrm{Im}[\Phi_2(l,k,r)]), \\ q_l(k,r) = \sqrt{|\epsilon(k)| + 1} r^{\varkappa_l - 1} (\mathrm{Im}[\Phi_1(l,k,r)] - \lambda^-_{uq}(l,k) \mathrm{Re}[\Phi_2(l,k,r)]), \end{cases} \tag{68}$$

while the corresponding matching coefficients contain now triplets $\lambda^-_{i,uq}(l,k)$, $i = 1, 2, 3$, which belong to three intervals $0 \le k \le k_1, k_1 \le k \le k_2$, and $k_2 \le k \le \infty$ and take the following form:

$$\begin{cases} \lambda^-_{1,uq}(l,k) = \dfrac{\sqrt{|(1-\epsilon)(\epsilon + V_0 + 1)|} J_{l+1/2}(\xi R) \mathrm{Im}[\Phi_1] + \sqrt{|(1+\epsilon)(\epsilon + V_0 - 1)|} J_{l+3/2}(\xi R) \mathrm{Re}[\Phi_1]}{\sqrt{|(1-\epsilon)(\epsilon + V_0 + 1)|} J_{l+1/2}(\xi R) \mathrm{Re}[\Phi_2] - \sqrt{|(1+\epsilon)(\epsilon + V_0 - 1)|} J_{l+3/2}(\xi R) \mathrm{Im}[\Phi_2]}, \\ \lambda^-_{2,uq}(l,k) = \dfrac{\sqrt{|(1-\epsilon)(\epsilon + V_0 + 1)|} I_{l+1/2}(\tilde{\xi} R) \mathrm{Im}[\Phi_1] - \sqrt{|(1+\epsilon)(\epsilon + V_0 - 1)|} I_{l+3/2}(\tilde{\xi} R) \mathrm{Re}[\Phi_1]}{\sqrt{|(1-\epsilon)(\epsilon + V_0 + 1)|} I_{l+1/2}(\tilde{\xi} R) \mathrm{Re}[\Phi_2] + \sqrt{|(1+\epsilon)(\epsilon + V_0 - 1)|} I_{l+3/2}(\tilde{\xi} R) \mathrm{Im}[\Phi_2]}, \\ \lambda^-_{3,uq}(l,k) = \dfrac{\sqrt{|(1-\epsilon)(\epsilon + V_0 + 1)|} J_{l+1/2}(\xi R) \mathrm{Im}[\Phi_1] - \sqrt{|(1+\epsilon)(\epsilon + V_0 - 1)|} J_{l+3/2}(\xi R) \mathrm{Re}[\Phi_1]}{\sqrt{|(1-\epsilon)(\epsilon + V_0 + 1)|} J_{l+1/2}(\xi R) \mathrm{Re}[\Phi_2] + \sqrt{|(1+\epsilon)(\epsilon + V_0 - 1)|} J_{l+3/2}(\xi R) \mathrm{Im}[\Phi_2]}. \end{cases} \tag{69}$$

On the rhs of (69), $\epsilon \equiv \epsilon(k) < -1, \xi = \xi(k), \tilde{\xi} = \tilde{\xi}(k)$, and $R = R(Z)$, the parameters b and c of Kummer's functions are defined in (54), but with negative $\epsilon(k) < -1$, while the arguments in the functions Φ_1 and Φ_2 remain the same as in (58).

The phase shifts $\delta^-_{uq}(l,k)$ are given by the same expressions (59)–(61) as for the upper one with two main differences. First, $\epsilon(k)$ is negative and, second, the matching coefficients are defined via (69) in accordance with three intervals $0 \le k \le k_1, k_1 \le k \le k_2$, and $k_2 \le k \le \infty$.

The calculation of phase shifts for the region $l + 1 < Q$, that means for imaginary $\varkappa_l$, proceeds as follows. The inner solutions for $r \le R(Z)$ remain unchanged, while for $r \ge R(Z)$ the scattering states of the DC problem can be written now in terms of the Kummer $\Phi(b,c,z)$ and conjugated Kummer $\Phi^*(b,c,z)$ ones, since for imaginary $\varkappa_l$ the Kummer relation does not destroy the independence of solutions built in such a way.

Upon introducing the notation

$$\varkappa_l = i\eta_l, \tag{70}$$

where

$$\eta_l = \sqrt{Q^2 - (l+1)^2}, \tag{71}$$

and the parameters b and c of Kummer's functions in the form

$$b_l = i(\eta_l - \epsilon(k) Q/k), \qquad c_l = 1 + 2i\eta_l, \tag{72}$$

the real-valued scattering solution for the (u_l, q_l) pair in the upper continuum is represented as

$$\begin{cases} u_l(k,r) = \frac{1}{r}\sqrt{\epsilon(k)+1}\mathrm{Re}[e^{ik(r-R)}(\frac{r}{R})^{i\eta_l}N_R^*(l,k)F_1(l,k,r)], \\ q_l(k,r) = \frac{1}{r}\sqrt{\epsilon(k)-1}\mathrm{Im}[e^{ik(r-R)}(\frac{r}{R})^{i\eta_l}N_R^*(l,k)F_2(l,k,r)], \end{cases} \tag{73}$$

where

$$\begin{aligned} F_1(l,k,r) &= b_l\Phi(b_l+1,c_l,-2ikr) + (l+1+iQ/k)\Phi(b_l,c_l,-2ikr), \\ F_2(l,k,r) &= b_l\Phi(b_l+1,c_l,-2ikr) - (l+1+iQ/k)\Phi(b_l,c_l,-2ikr), \end{aligned} \tag{74}$$

and

$$N_R(l,k) = \sqrt{(\epsilon-1)(\epsilon+V_0+1)}J_{l+1/2}(\xi R)F_{2R} + i\sqrt{(\epsilon+1)(\epsilon+V_0-1)}J_{l+3/2}(\xi R)F_{1R}. \tag{75}$$

On the rhs of (75), $\epsilon \equiv \epsilon(k) = +\sqrt{k^2+1} \geq 1, \xi = \xi(k)$, and $R = R(Z)$ with the same set of arguments $(l,k,R(Z))$ in functions F_{1R} and F_{2R}.

From (73)–(75) for the phase shift $\delta_{uq}^+(l,k)$, one finds

$$\delta_{uq}^+(l,k) = \frac{\pi l}{2} + \frac{\epsilon(k)Q}{k}\ln(2kr) + \mathrm{Arg}[C(l,k)], \tag{76}$$

where

$$C(l,k) = i\left[e^{-\pi\eta_l/2}\tilde{N}_R(l,k)\left(\frac{\Gamma(c_l)}{\Gamma(b_l)}\right)^* + e^{\pi\eta_l/2}\tilde{N}_R^*(l,k)(l+1+iQ/k)\frac{\Gamma(c_l)}{\Gamma(1+i(\eta_l+\epsilon(k)Q/k))}\right], \tag{77}$$

and

$$\tilde{N}_R(l,k) = e^{i(kR+\eta_l\ln(2kR))}N_R(l,k). \tag{78}$$

In the lower continuum with $\epsilon(k) < -1$, we again deal with three separate intervals $0 \leq k \leq k_1$, $k_1 \leq k \leq k_2$, and $k_2 \leq k \leq \infty$. The general answer for scattering solutions in this case reads

$$\begin{cases} u_l(k,r) = \frac{1}{r}\sqrt{|\epsilon(k)|-1}\mathrm{Im}[e^{ik(r-R)}(\frac{r}{R})^{i\eta_l}N_R^*(l,k)F_1(l,k,r)], \\ q_l(k,r) = \frac{1}{r}\sqrt{|\epsilon(k)|+1}\mathrm{Re}[e^{ik(r-R)}(\frac{r}{R})^{i\eta_l}N_R^*(l,k)F_2(l,k,r)], \end{cases} \tag{79}$$

where

$$N_R(l,k) = \begin{cases} \sqrt{|(1+\epsilon)(\epsilon+V_0-1)|}J_{l+3/2}(\xi R)F_{1R} + i\sqrt{|(1-\epsilon)(\epsilon+V_0+1)|}J_{l+1/2}(\xi R)F_{2R}, & 0 \leq k \leq k_1, \\ \sqrt{|(1+\epsilon)(\epsilon+V_0-1)|}I_{l+3/2}(\tilde{\xi} R)F_{1R} - i\sqrt{|(1-\epsilon)(\epsilon+V_0+1)|}I_{l+1/2}(\tilde{\xi} R)F_{2R}, & k_1 \leq k \leq k_2, \\ \sqrt{|(1+\epsilon)(\epsilon+V_0-1)|}J_{l+3/2}(\xi R)F_{1R} - i\sqrt{|(1-\epsilon)(\epsilon+V_0+1)|}J_{l+1/2}(\xi R)F_{2R}, & k_2 \leq k \leq \infty. \end{cases} \tag{80}$$

From (79) and (80), for the phase shift one finds

$$\delta_{uq}^-(l,k) = \frac{\pi l}{2} + \frac{\epsilon(k)Q}{k}\ln(2kr) + \mathrm{Arg}[D(l,k)], \tag{81}$$

where

$$D(l,k) = e^{\pi\eta_l/2}\tilde{N}_R^*(l,k)(l+1+iQ/k)\frac{\Gamma(c_l)}{\Gamma(1+i(\eta_l+\epsilon(k)Q/k))} - e^{-\pi\eta_l/2}\tilde{N}_R(l,k)\left(\frac{\Gamma(c_l)}{\Gamma(b_l)}\right)^*. \tag{82}$$

Finally, the total elastic phase $\delta_{\rm tot}(l,k)$ is obtained by summing up all the four separate phases for (u_l, q_l) and (p_l, v_l) pairs

$$\delta_{\rm tot}(l,k) = \delta^{+}_{uq}(l,k) + \delta^{-}_{uq}(l,k) + \delta^{+}_{pv}(l,k) + \delta^{-}_{pv}(l,k), \tag{83}$$

where $\delta^{\pm}_{pv}(l,k)$ are obtained from $\delta^{\pm}_{uq}(l,k)$ via the crossing-symmetry prescription. $\delta_{\rm tot}(l,k)$ automatically includes contributions from both continua and both parities and reveals the following general properties. First, each separate phase in (83) is determined from the asymptotics of scattering solutions only up to the additional term πs. Therefore, the term $2\pi l$ in $\delta_{\rm tot}(l,k)$ can be freely replaced by any other $2\pi s$ and so should be chosen by means of additional grounds, the main of which is $\delta_{\rm tot}(l, k\to\infty)\to 0$. Second, the Coulomb logarithms $\pm Q(|\epsilon|/k)\ln(2kr)$, which enter each separate phase, in the total phase cancel each other. However, after canceling Coulomb logarithms, the separate phase shifts contain still the singularities for both $k\to 0$ and $k\to\infty$. In particular, for $k\to\infty$ in the asymptotics of separate phases there remain the singular terms $\mp Q|\epsilon|\ln(2kR)/k$, but they also cancel mutually in the total phase just as in the $2+1$-dimensional case [24,30]. As a result, $\delta_{\rm tot}(l,k\to\infty)$ shows up for any $\varkappa_l$ the following vanishing asymptotics[1]:

$$\delta_{\rm tot}(l,k\to\infty) = \frac{1}{(kR)^3}\left[\frac{4}{3}Q^2((l+1)^2-3R^2) - (l+1)Q\sin(2Q)\cos(2kR-\pi l)\right] + O\left(\frac{1}{(kR)^4}\right). \tag{84}$$

As it was already stated above in Sec. III, the leading $O(1/(kR)^3)$ nonoscillating term of $\delta_{\rm tot}(l,k\to\infty)$ coincides exactly with the leading-order WKB asymptotics (36), while the oscillating ones in $\delta_{\rm tot}(l,k\to\infty)$ are responsible for diffraction on a sphere of the radius R. It would be also worthwhile to notice that the explicit asymptotics (84) confirms that the total phase is an even function of Q, but not of Z, since the dependence on Z includes also the function $R(Z)$.

The IR asymptotics of separate phases contain also the singularities of the form $\pm Q(1-\ln(Q/k))/k$. These singularities again cancel each other in $\delta_{\rm tot}(l,k\to 0)$, and so the total phase for $k\to 0$ possesses a finite limit, which for large $l\gg Q$ coincides with the WKB approximation and reproduces the answer for a pointlike source, but in a general case turns out to be quite different, especially for imaginary $\varkappa_l$. The explicit expressions for $\delta_{\rm tot}(l,k\to 0)$ depend strongly on whether $\varkappa_l$ is real or imaginary. In the case of real $\varkappa_l$ by means of the subsidiary functions

$$f_l = \frac{J_{2\varkappa_l}(\sqrt{8QR})[z_0 j_1 - (l+1+\varkappa_l)j_2] + j_2\sqrt{2QR}J_{1+2\varkappa_l}(\sqrt{8QR})}{J_{-2\varkappa_l}(\sqrt{8QR})[z_0 j_1 - (l+1-\varkappa_l)j_2] + j_2\sqrt{2QR}J_{1-2\varkappa_l}(\sqrt{8QR})},$$
$$g_l = \frac{J_{2\varkappa_l}(\sqrt{8QR})[(l+1-\varkappa_l)j_1 - z_0 j_2] + j_1\sqrt{2QR}J_{1+2\varkappa_l}(\sqrt{8QR})}{J_{-2\varkappa_l}(\sqrt{8QR})[(l+1+\varkappa_l)j_1 - z_0 j_2] + j_1\sqrt{2QR}J_{1-2\varkappa_l}(\sqrt{8QR})}, \tag{85}$$

where

$$z_0 = \sqrt{Q^2+2QR}, \qquad j_1 = J_{l+1/2}(z_0), \qquad j_2 = J_{l+3/2}(z_0), \tag{86}$$

the answer for $\delta_{\rm tot}(l,k\to 0)$ reads

$$\tan\left(\delta_{\rm tot}(l,k\to 0)\right) = \tan\{\mathrm{Arg}[(1-e^{2\pi i\varkappa_l}f_l)(1-e^{2\pi i\varkappa_l}g_l)] - 2\pi\varkappa_l\}. \tag{87}$$

At the same time, for imaginary $\varkappa_l = i\eta_l$ by means of two subsidiary phases,

$$\varphi_l = -\mathrm{Arg}\left\{\sqrt{1+V_0/2}j_1 2QJ_{2i\eta_l}\left(\sqrt{8QR}\right) + \sqrt{2V_0}j_2\left[\sqrt{2QR}J_{1+2i\eta_l}\left(\sqrt{8QR}\right) - \left(l+1+i\eta_l\right)J_{2i\eta_l}\left(\sqrt{8QR}\right)\right]\right\},$$
$$\chi_l = -\mathrm{Arg}\left\{\sqrt{2V_0}j_1\left[\sqrt{2QR}J_{1+2i\eta_l}\left(\sqrt{8QR}\right) + \left(l+1-i\eta_l\right)J_{2i\eta_l}\left(\sqrt{8QR}\right)\right] - \sqrt{1+V_0/2}j_2 2QJ_{2i\eta_l}\left(\sqrt{8QR}\right)\right\}, \tag{88}$$

instead of (87) one finds

[1]Here there is shown only the leading order of the asymptotical expansion of $\delta_{\rm tot}(l,k\to\infty)$ in inverse powers of kR. At the same time, by means of computer algebra tools, it is possible to derive in explicit form as many orders of this expansion as needed. It is quite important, since for concrete calculation of the phase integral such explicit terms of asymptotics are very useful, because it allows one to perform the integration over large k in the phase integral with given accuracy purely analytically.

$$\tan\left(\delta_{\rm tot}(l,k\to 0)\right) = \tan\{\mathrm{Arg}[(e^{\pi\eta_l+i\varphi_l}-e^{-\pi\eta_l-i\varphi_l})(e^{\pi\eta_l+i\chi_l}-e^{-\pi\eta_l-i\chi_l})]\}. \tag{89}$$

The peculiar feature in the behavior of $\delta_{\rm tot}(l,k)$ is the appearance of (positronic) elastic resonances upon diving of each subsequent discrete level into the lower continuum. Here it should be noted that the additional πs in the separate phase shifts, mentioned above, are in principle unavoidable, since this arbitrariness comes from the possibility to alter the common factor in the corresponding wave functions. So one needs to apply a special procedure, which provides the means to distinguish between such artificial jumps in the phases by π of purely mathematical origin in the inverse tan function, and the physical ones, which are caused by resonances and for extremely narrow low-energy resonances look just like the same jumps by π. Removing the first ones, coming from the inverse tan function, we provide the continuity of the phases, while the latter contain an important physical information. Hence, no matter how narrow they might be, they must necessarily be preserved in the phase function, and so this procedure should be performed with a very high level of accuracy.

In Fig. 2, the pertinent set of total phase curves for $Z=300$ is shown. For such Z only the four first levels from the s channel have already dived into the lower continuum, namely, $1s_{1/2}(Z_{\rm cr,1}\simeq 173.6), 2p_{1/2}(Z_{\rm cr,2}\simeq 188.5)$, $2s_{1/2}(Z_{\rm cr,3}\simeq 244.3)$, and $3p_{1/2}(Z_{\rm cr,4}\simeq 270.5)$.[2] So for $Z=300$ it is only the s channel, where $\delta_{\rm tot}(l,k)$ undergoes corresponding resonant jumps by π. It should be remarked, however, that each $Z_{{\rm cr},i}$ given above corresponds to the case of an external Coulomb source with charge $Z=Z_{{\rm cr},i}$ and radius $R_i=R(Z_{{\rm cr},i})$. Hence, this is not exactly the case under consideration with $Z=300$ and $R(Z=300)$ fixed; rather it is a qualitative picture of what happens with the first four lowest s levels in this case. They are absent in the discrete spectrum and show up as positronic resonances, the rough disposition of which can be understood as a result of diving of corresponding levels at $Z_{{\rm cr},i}$. However, their exact positions on the k axis can be found only via thorough restoration of the form of $\delta_{\rm tot}(0,k)$.

In particular, the two first low-energy narrow jumps in Fig. 2(a) correspond to resonances that are caused by diving of $2s_{1/2}$ and $3p_{1/2}$, which happens quite close to $Z=300$. At the same time, the jumps caused by diving of $1s_{1/2}$ and $2p_{1/2}$ have been already gradually smoothed and almost merged together; hence they look like one big 2π jump, which is already significantly shifted to the region of larger k. In the other channels with $l\geq 1$, there are no diving levels for such Z and so $\delta_{\rm tot}(l,k)$ in these channels look like a decreasing function, whose behavior roughly resembles the one of the WKB phase up to an oscillating tail.

In Fig. 3 the behavior of total phases in pertinent channels is presented for $Z=600$. For such Z, diving of discrete levels occurs already up to $l=3$. The dived levels naturally group into pairs containing states of different parity. For $l=0$ these are $\{1s_{1/2},2p_{1/2}\},\ldots,\{5s_{1/2},6p_{1/2}\}$ and the last unpaired $6s_{1/2}$ with corresponding $Z_{\rm cr}\simeq 576.4$. For $l=1$ it is the set $\{2p_{3/2},3d_{3/2}\},\ldots,\{5p_{3/2},6d_{3/2}\}$ with the last unpaired $6p_{3/2}(Z_{\rm cr}\simeq 581.2)$, while for $l=2$ one has $\{3d_{5/2},4f_{5/2}\},\ldots,\{5p_{3/2},6f_{5/2}\}$ with the last $6f_{5/2}(Z_{\rm cr}\simeq 564.5)$. Diving stops at $l=3$ with the pair $\{4f_{7/2},5g_{7/2}\}$, corresponding to critical charges $\simeq$578.6 and $\simeq$582.7. The meaning of $Z_{{\rm cr},i}$ in this case is the same as for $Z=300$. The behavior of total phases in these channels differs only by the number of resonant jumps from the s channel for $Z=300$, therefore in the appearance of curves. For the s channel, the total number of dived levels exceeds 11, and $\delta_{\rm tot}(0,k)$ undergoes the corresponding number of jumps by π, which at small k practically overlap each other. At the same time, for $l=2$ and $l=3$ all the jumps are quite clearly pronounced, transparent, and lie in one-to-one correspondence with the sequence of dived levels. In the other channels with $l\geq 4$ there are no dived levels and so the behavior of $\delta_{\rm tot}(l,k)$ is quite similar to those from $Z=300$ with $l\geq 1$.

In the discrete spectrum, it also suffices to consider only the (u_l,q_l) pair, since the contribution of the (p_l,v_l) pair can be again achieved via crossing symmetry of the initial DC problem. For the external potential (1), the discrete levels with $|\epsilon|<1$ are found via equations written in terms of the Tricomi function $\Psi(b,c,z)$, which are valid for any $\varkappa_l$. By means of denotations,

$$\gamma=\sqrt{1-\epsilon^2},\quad b_l=\varkappa_l-\epsilon Q/\gamma,\quad c_l=1+2\varkappa_l,$$
$$\Psi=\Psi(b_l,c_l,2\gamma R),\quad \Psi_+=\Psi(b_l+1,c_l,2\gamma R), \tag{90}$$

and

$$\xi=\sqrt{(\epsilon+V_0)^2-1}, \tag{91}$$

the equation for (u_l,q_l) levels reads

$$(l+1-Q/\gamma)\frac{\Psi_+}{\Psi}=\frac{\sqrt{(1+\epsilon)(\epsilon+V_0-1)}J_{l+3/2}(\xi R)-\sqrt{(1-\epsilon)(\epsilon+V_0+1)}J_{l+1/2}(\xi R)}{\sqrt{(1+\epsilon)(\epsilon+V_0-1)}J_{l+3/2}(\xi R)+\sqrt{(1-\epsilon)(\epsilon+V_0+1)}J_{l+1/2}(\xi R)}. \tag{92}$$

[2]Such $Z_{{\rm cr},i}$ are determined from (96) with $R(Z)$ defined as in (101).

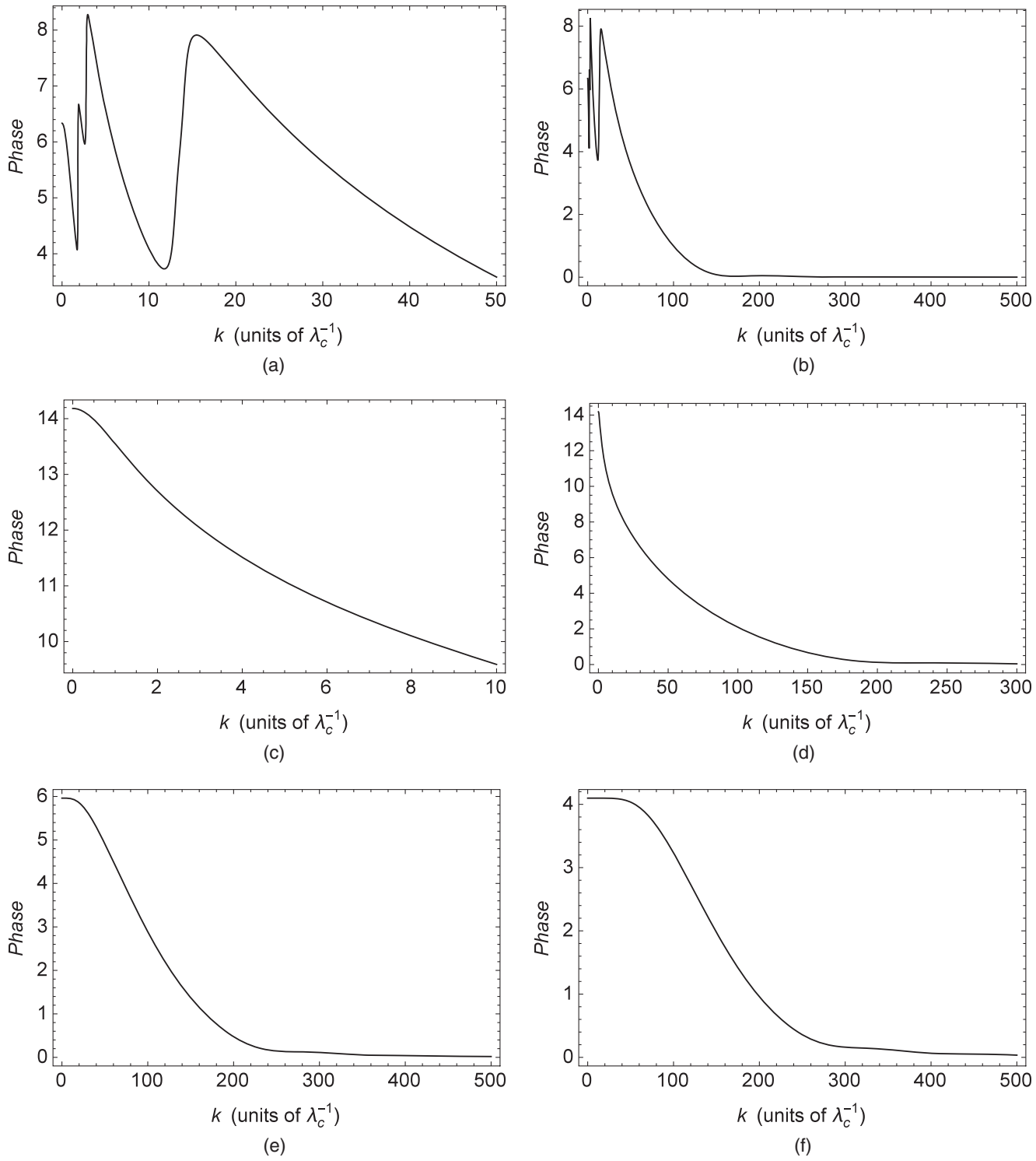

FIG. 2. $\delta_{\mathrm{tot}}(l,k)$ for $Z=300$ and (a),(b) $l=0$; (c),(d) $l=1$; (e) $l=2$; (f) $l=3$.

However, for imaginary $\varkappa_l = i\,\eta_l$, another form of equations turns out to be more pertinent for concrete calculations, since it deals with the Kummer function instead of the Tricomi one

$$\frac{\mathrm{Im}[X_l b_l \Phi_+]}{\mathrm{Im}[X_l \Phi]} = (l+1+Q/\gamma)\,\frac{\sqrt{(1-\epsilon)(\epsilon+V_0+1)}J_{l+1/2}(\xi R) - \sqrt{(1+\epsilon)(\epsilon+V_0-1)}J_{l+3/2}(\xi R)}{\sqrt{(1-\epsilon)(\epsilon+V_0+1)}J_{l+1/2}(\xi R) + \sqrt{(1+\epsilon)(\epsilon+V_0-1)}J_{l+3/2}(\xi R)}, \tag{93}$$

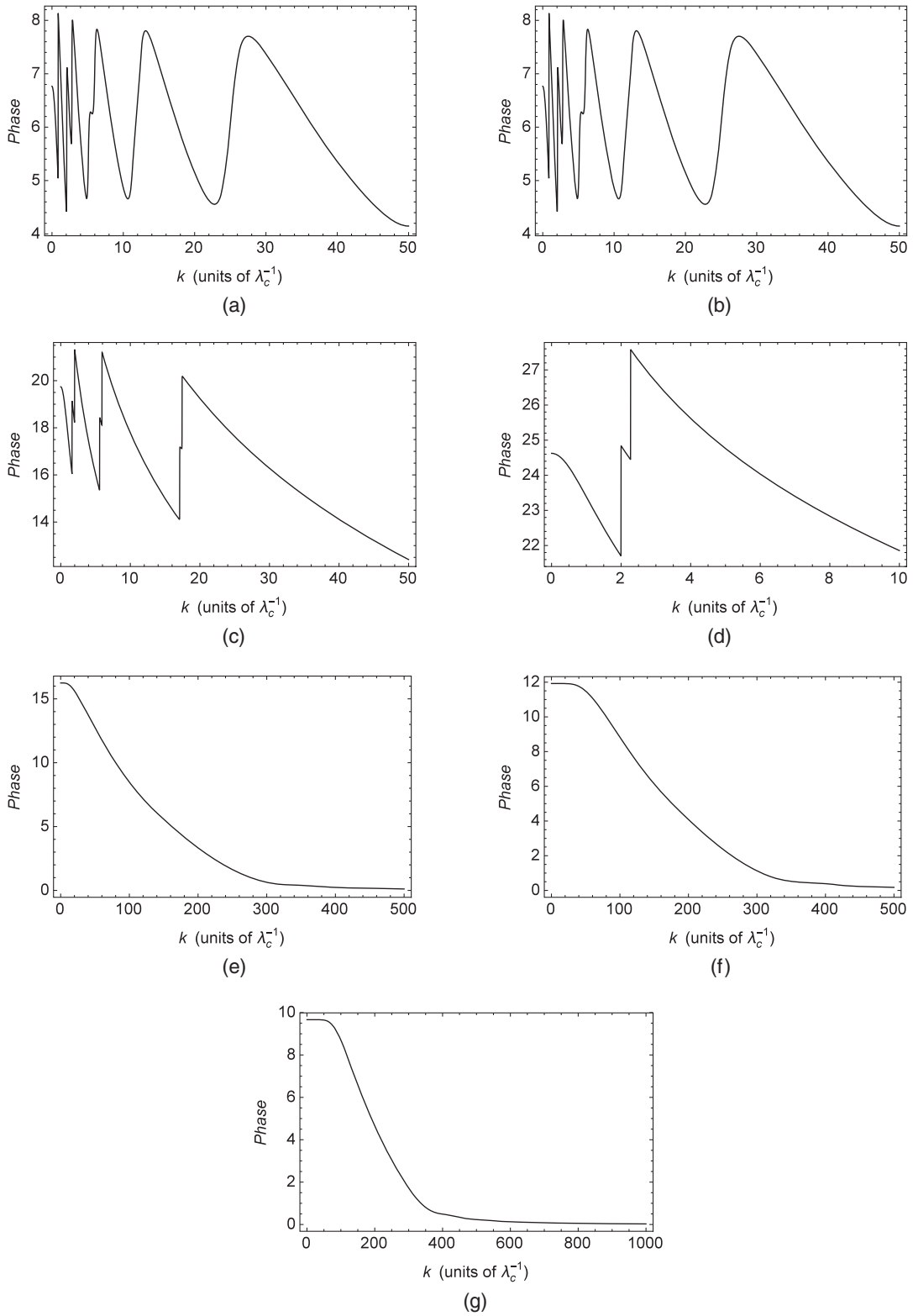

FIG. 3. $\delta_{\mathrm{tot}}(l,k)$ for $Z=600$ and (a) $l=0$, (b) $l=1$, (c) $l=2$, (d) $l=3$, (e) $l=4$, (f) $l=5$, (g) $l=6$.

where

$$b_l = i\eta_l - \epsilon Q/\gamma, \qquad c_l = 1 + 2i\eta_l,$$
$$\Phi = \Phi(b_l, c_l, 2\gamma R), \qquad \Phi_+ = \Phi(b_l + 1, c_l, 2\gamma R), \quad (94)$$

and

$$X_l = \mathrm{e}^{i\eta_l \ln(2\gamma R)} \frac{\Gamma(b_l)}{\Gamma(c_l)}, \quad (95)$$

with the same γ and ξ.

Discrete levels on the threshold of the lower continuum with $\epsilon = -1$ are directly connected with the corresponding critical charges $Z_{\mathrm{cr},i}$ of the external source and so are the subject of another procedure, which deals specially with this case. For details see, e.g., Ref. [4]. The result is that such levels appear only for $\varkappa_l = i\eta_l$, while the critical charges for both parities ($\pm$) are found in this case from equations

$$2z_1 K_{2i\eta_l}\left(\sqrt{8QR}\right) J_\pm \mp \left[\sqrt{2QR}\left(K_{1+2i\eta_l}\left(\sqrt{8QR}\right) + K_{1-2i\eta_l}\left(\sqrt{8QR}\right)\right) \pm 2(l+1)K_{2i\eta_l}\left(\sqrt{8QR}\right)\right] J_\mp = 0, \quad (96)$$

where $K_\nu(z)$ is the McDonald function, η_l is defined in (71), and

$$z_1 = \sqrt{Q^2 - 2QR},$$
$$J_+ = J_{l+3/2}(z_1), \qquad J_- = J_{l+1/2}(z_1). \quad (97)$$

The meaning of Eqs. (96) and (97) is twofold. First, for the given charge Z and $R = R(Z)$ by means of these equations, the existence of levels with $\epsilon = -1$ can be checked. The answer is positive if and only if the current Z coincides with one of $Z_{\mathrm{cr},i}$, otherwise there are no levels at the lower threshold. Second, by solving these equations with respect to Z and $R = R(Z)$, one finds the complete set of critical charges $Z_{\mathrm{cr},i}$.

The asymptotical behavior of the discrete spectrum for both (u_l, q_l) and (p_l, v_l) pairs in the vicinity of the condensation point $\epsilon_{n,l} \to 1$ reproduces the Coulomb-Schrödinger problem for a pointlike source with the same Z including $O(Q^4)$ fine-structure correction and $O(Q^{2l+4})$ correction coming from the nonvanishing size of the Coulomb source

$$1 - \epsilon_{n_r,l} = \frac{Q^2}{2(n_r + l + 1)^2} + Q^4\left(\frac{1}{2(l+1)(n_r + l + 1)^3} - \frac{3}{8(n_r + l + 1)^4}\right) - \frac{Q^2}{(n_r + l + 1)^2}\left(\frac{2QR}{n_r + l + 1}\right)^{2l+2} \frac{(n_r + 2l + 1)!}{n_r!} \frac{(2l+2)(2l+3)}{(2l+3)!^2}, \quad n_r \to \infty. \quad (98)$$

For any l in this asymptotics, the terms with Bohr levels and fine-structure correction are exactly summable over n_r starting from certain n_0 via

$$\sum_{n_r=n_0}^{\infty} \frac{1}{(n_r + a)^2} = \psi^{(1)}(n_0 + a),$$
$$\sum_{n_r=n_0}^{\infty} \frac{1}{(n_r + a)^3} = -\frac{1}{2}\psi^{(2)}(n_0 + a),$$
$$\sum_{n_r=n_0}^{\infty} \frac{1}{(n_r + a)^4} = \frac{1}{6}\psi^{(3)}(n_0 + a), \quad (99)$$

where $\psi^{(n)}(z) = d^n\psi(z)/dz^n$ and $\psi(z) = \Gamma'(z)/\Gamma(z)$. The correction from the nonzero size of the source in (98) is also exactly summable over $n_r \geq n_0$ in terms of $\psi^{(n)}(n_0 + a)$, but the general answer for arbitrary l is very cumbersome.

Thus, for any l, the global strategy of summation over the discrete spectrum in order to find its contribution to the partial $\mathcal{E}_{\mathrm{VP},l}(Z)$ turns out to be the following. Summation is performed separately for (u_l, q_l) and (p_l, v_l) pairs. In the first step for each pair, one finds the set of lowest levels with $n_r < n_0(l)$, where $n_0(l)$ is the subject of the condition that for $n_r \geq n_0(l)$ the levels coincide with the asymptotics (98) with a given accuracy. Since $n_0(l)$ is always finite, summation over this part of the discrete spectrum poses no problems. In the next step, the remaining infinite part of the spectrum is summed up by means of (98) and (99). Proceeding this way, we find with given accuracy the sum

$$S(l) = \sum_{\pm} \sum_{-1 \leq \epsilon^{\pm}_{n,l} < 1} (1 - \epsilon^{\pm}_{n,l}), \quad (100)$$

which is the discrete spectrum contribution to the partial VP energy (25). It should be noted, however, that for small or even moderate l and especially for the case $l + 1 < Q$ with $\varkappa_l = i\eta_l$ accounting for nonzero size of the Coulomb source in this calculation takes care, since the more current Z and $R(Z)$, the more $n_0(l)$. In actual calculations up to $Z \simeq 1000$ the value of $n_0(l)$ exceeds thousands or even dozens of thousands, and since all the levels with

$n_r < n_0(l)$ must be found by solving the corresponding equations numerically, it takes some definite time.[3]

V. RENORMALIZED VP ENERGY FOR THE COULOMB SOURCE (1)

For greater clarity of results, we restrict this presentation to the case of charged sphere (1) on the interval $0 < Z < 600$ with the numerical coefficient in Eq. (4) chosen as[4]

$$R(Z) = 1.228935(2.5Z)^{1/3}\ \text{fm}. \tag{101}$$

On this interval of Z the main contribution comes from the partial channels with $l = 0, \ldots, 3$, in which a nonzero number of discrete levels has already reached the lower continuum. In Fig. 4 there are shown the specific features of partial phase integrals, partial sums over discrete levels, and renormalized partial VP energies.

As it follows from Fig. 4(a), phase integrals increase monotonically with growing Z and are always positive. The clearly seen bending, which is in fact nothing else but the negative jump in the derivative of the curve, for each channel starts when the first discrete level in this channel crosses the border of the lower continuum. The origin of this effect is the sharp jump by π in $\delta_{\text{tot}}(l,k)$ due to the resonance just born. In each l channel, such effect is the mostly pronounced for the first level diving, which takes place at $Z_{\text{cr},1} \simeq 173.6$ for $l = 0$, at $Z_{\text{cr},5} \simeq 307.4$ for $l = 1$, at $Z_{\text{cr},15} \simeq 442.7$ for $l = 2$, and at $Z_{\text{cr},26} \simeq 578.6$ for $l = 3$.

The subsequent levels diving leads also to jumps in the derivative of $I(l)$, but they turn out to be much less pronounced, since with increasing Z_{cr} there shows up the effect of "catalyst poisoning"—just below the threshold of the lower continuum for $Z = Z_{\text{cr}} + \Delta Z$ and $\Delta Z \ll Z_{\text{cr}}$, the resonance broadening and its rate of further diving into the lower continuum are exponentially slower in agreement with the well-known result [33], according to which the resonance width just under the threshold behaves like $\sim \exp(-\sqrt{Z_{\text{cr}}/\Delta Z})$. This effect leads to that for each subsequent resonance the region of the phase jump by π with increasing Z grows exponentially slower, and the derivative of the phase integral changes in the same way. If not for this effect, then every next level upon reaching the lower continuum would lead to the same negative jump in the derivative as the first one, and the phase integral curve in the overcritical region would have a continuously increasing negative curvature with all the ensuing

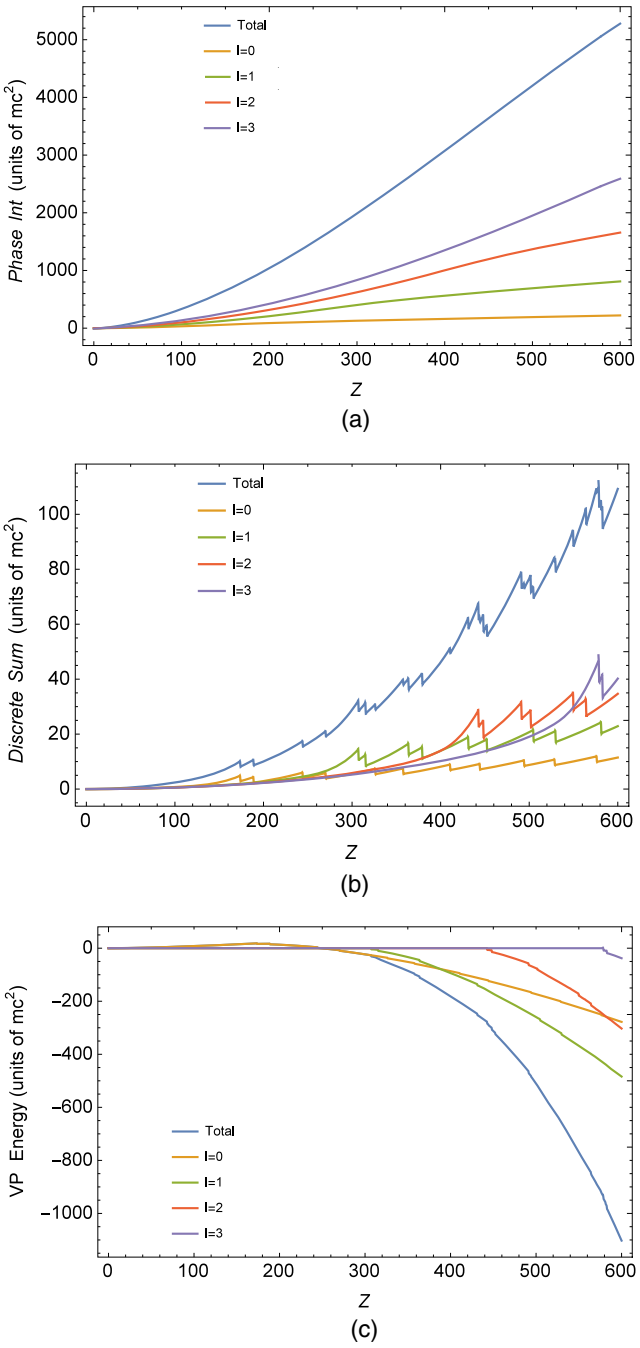

FIG. 4. $(l+1)I(l), (l+1)S(l), \mathcal{E}^{\text{ren}}_{\text{VP},l}(Z)$, and $I_{\text{tot}} = \sum_{l=0}^{3}(l+1)\times I(l), S_{\text{tot}} = \sum_{l=3}^{4}(l+1)S(l), \mathcal{E}^{\text{ren}}_{\text{VP,tot}}(Z) = \sum_{l=0}^{3}\mathcal{E}^{\text{ren}}_{\text{VP},l}(Z)$ on the interval $0 < Z < 600$.

[3]There exists another procedure of "quasiexact" summation over the discrete spectrum in such DC problems, which takes account of the nonzero size of the Coulomb source in an essentially nonperturbative way and therefore works much more rapidly. Within this approach, one needs to calculate exactly via Eqs. (92) and (93) only a few numbers, not more than 100 for reasonable accuracies lying in the interval 10^{-16}–10^{-20}, of the lowest levels lying below 0.99. Afterward the summation for the rest is performed in a closed form by means of (98) and (99), but already without the nonzero size correction. However, this method requires a thorough analysis of asymptotics of confluent hypergeometric functions in certain nontrivial regimes, combined with a number of additional original tricks, and so will be presented separately.

[4]With such a choice for a charged ball with $Z = 170$, the lowest $1s_{1/2}$ level lies precisely at $\epsilon_{1s} = -0.99999$. Furthermore, it is quite close to 1.23, which is the most commonly used coefficient in heavy nuclei physics.

consequences for the rate of decrease of $\mathcal{E}^{\rm ren}_{\rm VP}(Z)$. At the same time, before the first level diving the curves of $I(l)$ in all the partial channels reveal an almost quadratical growth. For the last channel with $l=3$ this growth takes place during almost the whole interval $0<Z<600$, since the first level diving in this channel occurs at $Z\simeq 578.6$, which is very close to $Z=600$ and simultaneously large enough already to be subject to the Zeldovich-Popov effect discussed just above.

The behavior of the total bound energy of discrete levels per each partial channel $S(l)$ is shown in Fig. 4(b). $S(l)$ are discontinuous functions with jumps emerging each time, when the charge of the source reaches the subsequent critical value and the corresponding discrete level dives into the lower continuum. At this moment the bound energy loses exactly two units of mc^2, which in the final answer must be multiplied by the degeneracy factor $l+1$. Because of this factor the jumps in the curves of $S(l)$ are more pronounced with growing l. On the intervals between two neighboring $Z_{\rm cr}$ the bound energy is always positive and increases monotonically, since there grow the bound energies of all the discrete levels, while on the intervals between $Z=0$ up to first level diving their growth is almost quadratic.

The partial VP energies $\mathcal{E}^{\rm ren}_{{\rm VP},l}(Z)$ are shown in Fig. 4(c). Note that the behavior of the s channel is different from the others, since in this channel the structure of the renormalization coefficient ζ_0 differs from those with $l\geq 1$ by the perturbative (Uehling) contribution to VP energy $\mathcal{E}^{(1)}_{\rm VP}(Z)$. It is indeed the latter term in the total VP energy that is responsible for an almost quadratic growth with Z of VP energy on the interval $0<Z<Z_{{\rm cr},1}$. The global change in the behavior of $\mathcal{E}^{\rm ren}_{{\rm VP},0}(Z)$ from the perturbative quadratic growth for $Z\ll Z_{{\rm cr},1}$, where the dominant contribution comes from $\mathcal{E}^{(1)}_{\rm VP}(Z)$, to the regime of decrease into the negative range with increasing Z beyond $Z_{{\rm cr},1}$ is shown below in Sec. VI in Figs. 5 and 6. At the same time, in the channels with $l\geq 1$ the quadratic perturbative contribution is absent. Therefore, upon renormalization (46)–(48), which removes the quadratic component in $I(l)$ and $S(l)$, just after first level diving $\mathcal{E}^{\rm ren}_{{\rm VP},l}(Z)$ reveal with increasing Z a well-pronounced decrease into the negative range.

To specify the dependence of partial VP energies $\mathcal{E}^{\rm ren}_{{\rm VP},l}(Z)$ on l below there are given Tables I and II with the required information. From these tables it is clearly seen that the main contribution to the total VP energy for a given Z is produced indeed by those partial channels, where a nonzero number of discrete levels has already reached the lower continuum. At the same time, the number of dived levels and their contribution to VP energy per partial channel do not correlate precisely. It is only the case of $Z=300$, when all the dived levels belong to the s channel, and indeed this channel dominates in $\mathcal{E}^{\rm ren}_{\rm VP}(Z)$. However, already for $Z=600$ the situation is different and with further growth of Z this discrepancy becomes more and more pronounced. Note also that vanishing of $\mathcal{E}^{\rm ren}_{{\rm VP},l}(Z)$ in the channels with l large enough to prevent levels diving proceeds even faster than predicted by WKB analysis performed in Sec. III.

The final answers for the total VP energy achieved this way are

$$\mathcal{E}^{\rm ren}_{\rm VP}(300)=-23.3,\qquad \mathcal{E}^{\rm ren}_{\rm VP}(600)=-1102.7. \tag{102}$$

For such Z the decrease of the total VP energy into the negative range proceeds very fast, but with further growth of Z the decay rate becomes smaller. In particular,

$$\mathcal{E}^{\rm ren}_{\rm VP}(1000)=-8398.6, \tag{103}$$

while the reasonable estimate of asymptotical behavior of $\mathcal{E}^{\rm ren}_{\rm VP}(Z)$ as a function of Z, achieved from the interval $1000<Z<3000$, reads

$$\mathcal{E}^{\rm ren}_{\rm VP}(Z)\sim -Z^4/R(Z). \tag{104}$$

TABLE I. Dependence of partial VP energies on l for $Z=300$ with and without multiplicity factor $l+1$.

l	0	1	2	3
$\mathcal{E}^{\rm ren}_{{\rm VP},l}(Z)$	−23.107040	−0.172432	−0.028663	−0.007796
$\mathcal{E}^{\rm ren}_{{\rm VP},l}(Z)/(l+1)$	−23.107040	−0.086216	−0.009554	−0.001949
Number of dived levels with multiplicity factor $2j+1$	8	0	0	0

TABLE II. Dependence of partial VP energies on l for $Z=600$ with and without multiplicity factor $l+1$.

l	0	1	2	3	4	5
$\mathcal{E}^{\rm ren}_{{\rm VP},l}(Z)$	−277.969408	−483.912426	−302.902746	−37.850795	−0.035715	−0.014984
$\mathcal{E}^{\rm ren}_{{\rm VP},l}(Z)/(l+1)$	−277.969408	−241.956213	−100.967582	−9.462698	−0.007143	−0.002497
Number of dived levels with multiplicity factor $2j+1$	22	36	36	16	0	0

It should be specially noted that the results (102)–(104) for the total VP energy are by no means something extraordinary. First, they correspond to the essentially nonperturbative region in effective coupling constant $Z\alpha$ in contrast to the perturbative one, where $\mathcal{E}^{(1)}_{\rm VP}$ is strictly positive. Furthermore, the values of $\mathcal{E}^{\rm ren}_{\rm VP}(Z)$ in Eqs. (102) and (103) should not be misleading, since the corresponding classical electrostatic self-energies $\mathcal{E}_{cl}(Z) = Z^2\alpha/2R(Z)$ are much larger, namely, 11361,36069, and 84505, while matching between $\mathcal{E}^{\rm ren}_{\rm VP}(Z)$ and $\mathcal{E}_{cl}(Z)$ takes place only at $Z \simeq 3000$, which is far beyond any reasonable charges of the Coulomb source.

Now let us consider the main differences in VP energy between the models of a uniformly charged sphere (1) and ball (2). Since they differ only by the shape of the potential inside the source, the general approach to evaluate the VP effects for the ball configuration, based on the techniques of the phase integral method and renormalization via fermionic loop, remains unchanged. The main difference is the structure of the inner solutions of the DC problem. In the case of the sphere, the latter can be found in analytical form, but for the ball such option is absent. In the last case, the most straightforward approach is to find numerically for given Z the inner solutions via direct solving of the corresponding DE. However, this turns out to be time consuming, since the inner solutions in the ball case are rapidly oscillating functions akin to Bessel-type ones, but with more complicated behavior, the calculation of which with the given accuracy takes time. However, for the potential (2) it is possible to apply another method, based on the approximation of the inner potential via a steplike function. Such approximation works quite well and already for a steplike function consisting of $100 < N < 1000$ segments yields the answer, which coincides with high precision with the exact numerical solution. The main advantage here is that the existing soft- and hardware nowadays is able to solve the appearing recurrences directly in analytical form and so avoids the problems with numerical solving of the DE. The details of such slicing of the ball are given in Appendix B.

Proceeding this way in the ball case, one obtains for $\delta_{\rm tot}(l,k)$ an analytical expression, which in explicit form looks quite cumbersome, but poses no problems for numerical evaluation in any point (l,k). Moreover, it can be easily verified by means of the WKB analysis, presented in Sec. III, that the leading-order asymptotics for $k \to \infty$ of the total phase for the ball remains $O(1/(kR)^3)$. IR asymptotics of $\delta_{\rm tot}(l,k)$ remains also finite, but now instead of compact explicit answers (87) and (89) for the sphere, it is given by quite lengthy expressions, which nevertheless allow for an effective numerical evaluation. So calculation of phase integrals (39) for the ball configuration by means of the steplike approximation can be implemented for any l without any serious loss of time and accuracy compared to the sphere.

Such slicing provides quite effective dealing with discrete levels in the ball case as well (for details see Appendix B). Further steps in order to find the total bound states contribution (100) to the partial VP energy (25) for the ball are the same as described above for the sphere.[5] The general behavior of $\mathcal{E}^{\rm ren}_{\rm VP}(Z)$ obtained this way for the ball configuration looks quite similar to that for the sphere with two main differences. The first one is that all the negative jumps in $\mathcal{E}^{\rm ren}_{\rm VP}(Z)$, caused by discrete levels diving into the lower continuum, are slightly shifted to the left. The second is that the general magnitude of VP energy in the ball case is approximately $(6/5) \times$ VP energy for the sphere. Remarkably enough, the same result (14) holds for the perturbative contributions $\mathcal{E}^{(1)}_{\rm VP}(Z)$ to VP energy under condition (12).

VI. SPONTANEOUS POSITRON EMISSION

Now let us consider more thoroughly the interval $10 \le Z \le 240$, when only the two first levels $1s_{1/2}$ and $2p_{1/2}$ with opposite parity ($\pm$) have already dived into the lower continuum at $Z_{\rm cr,1}$ and $Z_{\rm cr,2}$. This interval is of special interest, since indeed here lies the, nowadays, at least in principle, attainable region in heavy-ion collisions. The plots of fixed parity $\mathcal{E}^{\rm ren}_{\rm VP,\pm}(Z)$ for the charged sphere and ball source configurations are presented in Figs. 5 and 6.

The general approach (see Refs. [1–4] and citations therein), based on the framework [34], predicts that after discrete level diving into the lower continuum it transforms into a metastable state with lifetime $\sim 10^{-19}$ sec; afterward there should occur the spontaneous positron emission accompanied with vacuum shells formation. Such spontaneous emission of positrons should be provided solely by VP effects without any other channels of energy transfer. The corresponding positron spectra have been calculated first in Refs. [35,36] and were explored quite recently with more details in Refs. [9,11]. These spectra demonstrate, in particular, that the emission of low-energy positrons should be strongly suppressed by the repulsive interaction with the nuclei, while at high energy the spectra fall off exponentially.

In terms of $\mathcal{E}^{\rm ren}_{\rm VP}(Z)$, the energy balance suggests the following picture of this process. First, due to spherical symmetry of the source, all the angular quantum numbers and parity of the dived level are preserved by the metastable state and further by positrons created. The rest mass of positrons is created just after levels diving via negative jumps in VP energy at corresponding $Z_{{\rm cr},i}$, which are exactly equal to $2 \times mc^2$ in accordance with two possible spin projections. However, to create a real positron

[5]The procedure of quasiexact summation over the discrete spectrum in such DC problems, which takes into account the nonzero size of the Coulomb source in an essentially nonperturbative way, can be extended for the ball case too.

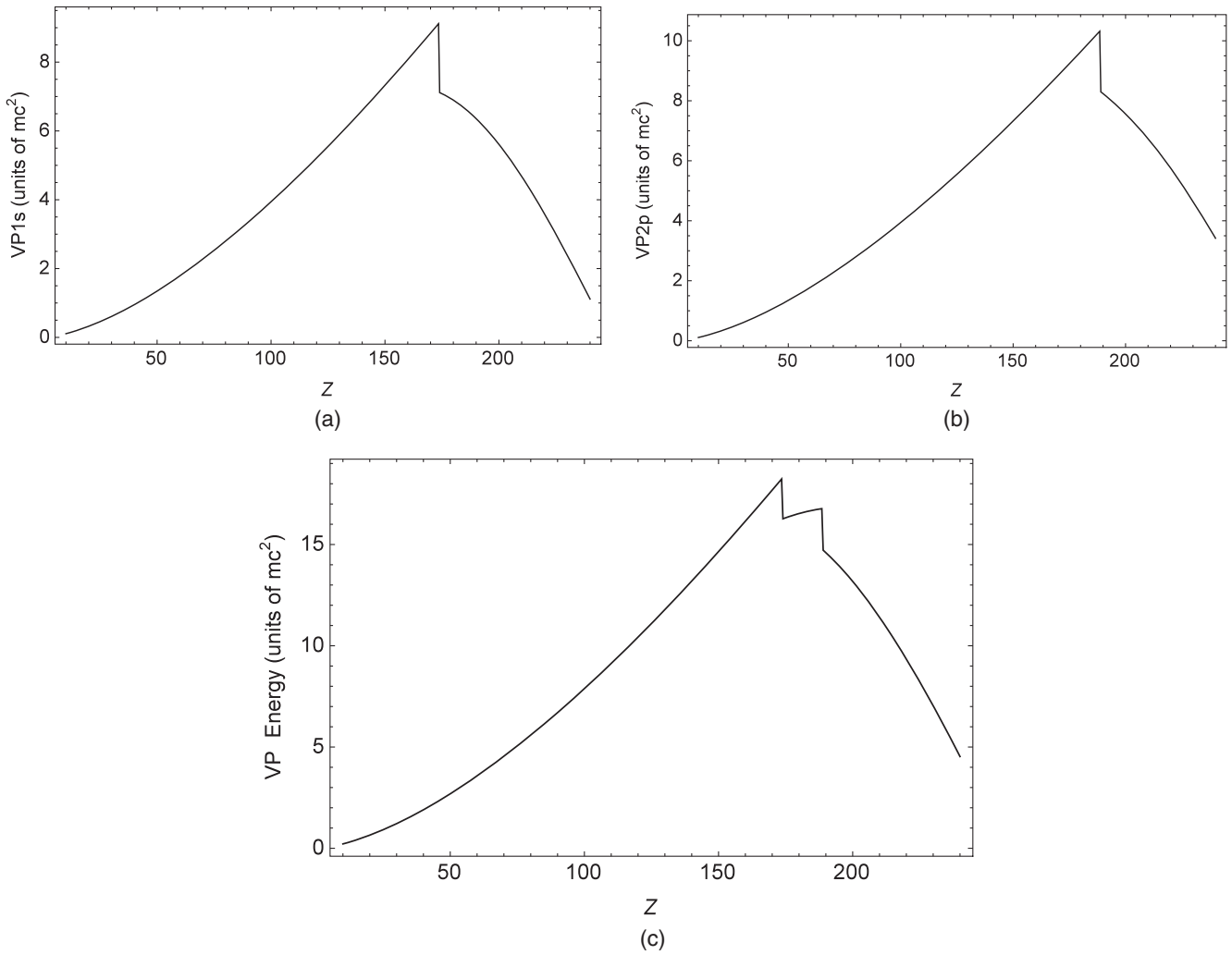

FIG. 5. a) $\mathcal{E}^{\mathrm{ren}}_{\mathrm{VP},+}(Z)$, b) $\mathcal{E}^{\mathrm{ren}}_{\mathrm{VP},-}(Z)$, c) $\mathcal{E}^{\mathrm{ren}}_{\mathrm{VP}}(Z)$on the interval $10 \le Z \le 240$ (sphere).

scattering state it is not enough due to repulsion between positrons and the Coulomb source. To supply the emerging vacuum positrons with corresponding potential energy, an additional decrease of $\mathcal{E}^{\mathrm{ren}}_{\mathrm{VP}}(Z)$ in each parity channel is required. So we are led to the following energy balance conditions for spontaneous positrons emission after level diving at $Z_{\mathrm{cr},i}$ for a given $Z > Z_{\mathrm{cr},i}$. In the even $1s$ case,

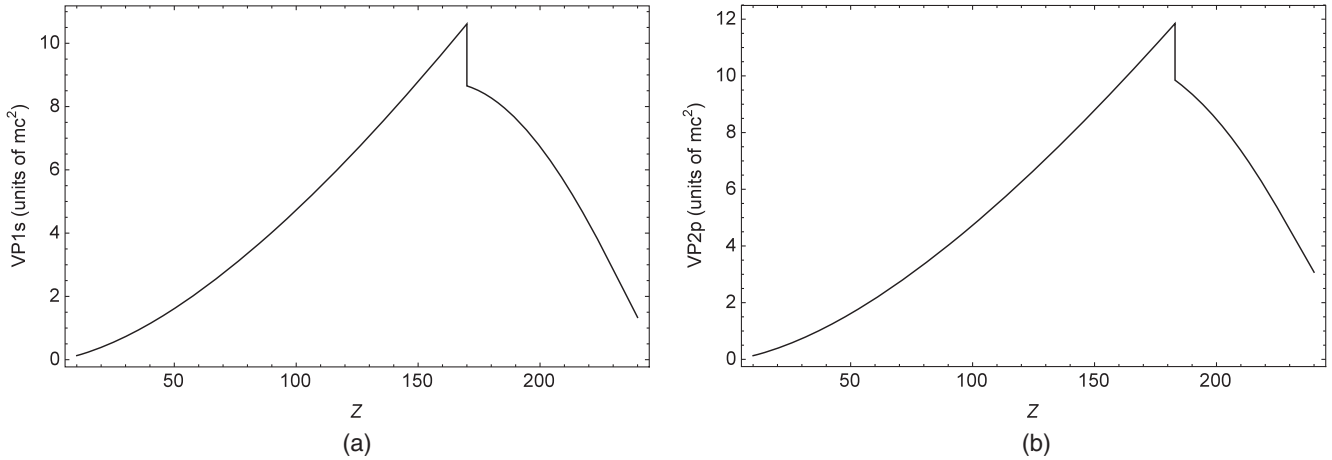

FIG. 6. a) $\mathcal{E}^{\mathrm{ren}}_{\mathrm{VP},+}(Z)$, b) $\mathcal{E}^{\mathrm{ren}}_{\mathrm{VP},-}(Z)$ on the interval $10 \le Z \le 240$ (ball).

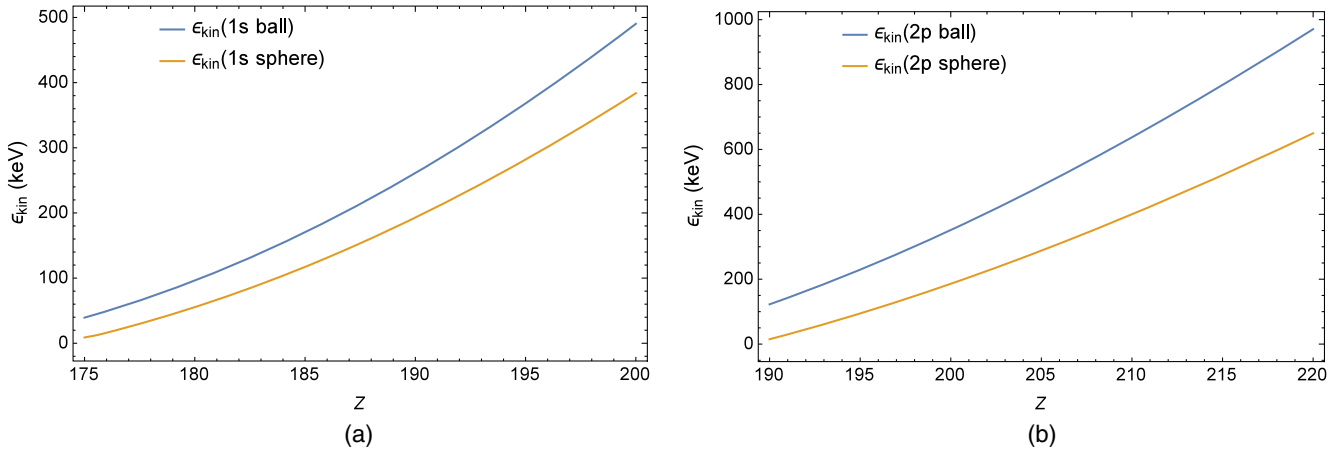

FIG. 7. $\epsilon_{\mathrm{kin}}(Z)$ with definite parity on the pertinent intervals of Z for sphere and ball source configurations and (a) $1s$ channel (even), (b) $2p$ channel (odd).

$$\mathcal{E}^{\mathrm{ren}}_{\mathrm{VP},+}(Z_{\mathrm{cr},1}+0)-\mathcal{E}^{\mathrm{ren}}_{\mathrm{VP},+}(Z)=2\epsilon^{+}_{\mathrm{kin}}(Z), \quad (105)$$

while in the odd $2p$ case,

$$\mathcal{E}^{\mathrm{ren}}_{\mathrm{VP},-}(Z_{\mathrm{cr},2}+0)-\mathcal{E}^{\mathrm{ren}}_{\mathrm{VP},-}(Z)=2\epsilon^{-}_{\mathrm{kin}}(Z), \quad (106)$$

where $\epsilon^{\pm}_{\mathrm{kin}}(Z)$ is the positron kinetic energy at the peak of resonance and it is assumed that for each parity positrons are created in pairs with opposite spin projections. $\mathcal{E}^{\mathrm{ren}}_{\mathrm{VP},\pm}(Z_{\mathrm{cr},i}+0)$ in (105) and (106) signifies that the rest mass of positrons $2\times mc^2$ is already created by the negative jump in $\mathcal{E}^{\mathrm{ren}}_{\mathrm{VP}}(Z)$, which takes place exactly at $Z_{\mathrm{cr},i}$.

It should be specially noted, that the relations (105) and (106) do not in any way mean that for a given $Z>Z_{\mathrm{cr},i}$ only positrons with such fixed energy can be emitted. Actually, they define the arguments of energetic δ functions in the well-known general quantum-mechanical expression for the metastable state decay rate

$$\gamma=\frac{2\pi}{\hbar}\sum_{f\neq i}|T_{fi}|^2\delta(E_f-E_i). \quad (107)$$

In the present case, the in-state is the metastable hole in the lower continuum with definite parity, created after corresponding discrete level diving, with energy $E_i=\mathcal{E}^{\mathrm{ren}}_{\mathrm{VP},\pm}(Z_{\mathrm{cr}}+0)-\mathcal{E}^{\mathrm{ren}}_{\mathrm{VP},\pm}(Z)>0$, while the final state contains two emitted positrons, whence $E_f=2\epsilon^{\pm}_{\mathrm{kin}}$. In agreement with Refs. [9,11], in the considered range of Z the spontaneous positrons are limited to the energy $0<\epsilon_{\mathrm{kin}}<800$ (see Fig. 7), while the related natural resonance widths do not exceed a few keV [37]. Note that, in the present spherically symmetric case, the widths of resonances can be found directly from the jumps by π in $\delta_{\mathrm{tot}}(l,k)$, considered in Sec. IV (see Figs. 2 and 3).

Now let us explore with more qualitative arguments the conditions for the most reliable vacuum positron detection on the nuclear conversion pairs background. To a large extent this issue is motivated by the nontrivial role of lepton number in such processes, since it is possible that either the lepton number conservation must be broken or the positron emission prohibited. Recent papers [9,11], aimed at the detailed study of spontaneous emission in slow heavy-ion collisions, have shown that one could expect a clear signal of transition to the supercritical mode for bare Cm nuclei with the highest $Z=96$, whose colliding trajectories are close to head-on ones. These results look quite promising, but one should keep in mind that the slow head-on collisions of charged particles are highly unstable with respect to deviations in the transverse plane. Meanwhile, the case under consideration in Refs. [9,11] implies the scenario of colliding beams with total number of particles not less than 10^6; hence the deviations of colliding trajectories due to interparticle interactions in the beam are inevitable. So one should expect that the most part of such slow collisions reduces to the peripheral ones, which cannot produce a clear signal distinguished from the nuclear conversion.

Another point of view is based on the treatment of spontaneous emission as a specific lepton pair creation, in which instead of a real electron there appears a vacuum shell with corresponding VP densities of charge and (presumably) of the lepton number. General properties of pair production [5,18] predict the natural scales for such processes as $\sim mc^2$ in energy and $\sim\hbar/mc$ in spatial extent. Therefore, it is useful to introduce the parameter d via the relation[6]

[6]Such d can be interpreted as the distance from the center of the Coulomb source and the conditional point of the vacuum positron creation, although the uncertainty relation inhibits any kind of spatial localization in the scattering state with fixed energy. However, such treatment of the parameter d turns out to be quite pertinent and, additionally, can be reliably justified at least in the quasiclassical approximation.

TABLE III. $Z^*_\pm(d)$ for $2/3 \le d \le 137$ (sphere).

d	2/3	1	2	3	4	5	7	10	20	50	80	100	137
$Z^*_{1s}(d)$	233.0	216.8	199.4	192.7	189.0	186.5	183.5	181.1	177.8	175.6	174.9	174.8	174.0
$Z^*_{2p}(d)$	243.4	227.1	209.6	203.3	200.0	198.0	195.6	193.7	191.4	189.9	189.6	189.0	188.8

TABLE IV. $Z^*_\pm(d)$ for $2/3 \le d \le 137$ (ball).

d	2/3	1	2	3	4	5	7	10	20	50	80	100	137
$Z^*_{1s}(d)$	224.0	210.3	194.8	188.6	185.1	182.8	180.0	177.6	174.3	171.9	171.2	171.0	170.7
$Z^*_{2p}(d)$	228.4	215.1	200.9	195.6	192.8	191.0	188.9	187.2	185.2	183.9	183.6	183.4	183.3

$$\epsilon_{\rm kin}(Z) = Z\alpha/d. \tag{108}$$

From the arguments presented above, there follows that the reasonable choice for d should be approximately one electron Compton length λ_C ($= 1$ in the units accepted). Moreover, λ_C is a reliable estimate from above for the average radius of vacuum shells, created together with the positron emission, in the considered range of Z ($\simeq$0.9 for $1s$ shell and $\simeq$0.6 for $2p$ shell for the charged sphere).

At the same time, performed calculations show that the spontaneous emission is quite sensitive to d. In particular, upon inverting Eqs. (105), (106), and (108) into the functions $Z^*_\pm(d)$, shown in Tables III and IV and Fig. 8, one finds that for $d \simeq 1$ the emission of positrons cannot occur earlier than Z exceeds $Z^*_{1s}(1) \simeq 217, Z^*_{2p}(1) \simeq 227$ (sphere), $Z^*_{1s}(1) \simeq 211, Z^*_{2p}(1) \simeq 215$ (ball) [to compare with $Z_{\rm cr,1} = 173.6, Z_{\rm cr,2} = 188.5$ (sphere), $Z_{\rm cr,1} = 170, Z_{\rm cr,2} = 183.1$ (ball)]. Note also that $Z^*_\pm(d)$ increase very rapidly for $d < \lambda_C$. In particular, already for $d = 2/3$ one obtains $Z^*_{1s}(2/3) \simeq 233, Z^*_{2p}(2/3) \simeq 244$ (sphere) and $Z^*_{1s}(2/3) \simeq 224, Z^*_{2p}(2/3) \simeq 229$ (ball). Such Z^* lie far beyond the interval $170 \le Z \le 192$, which is nowadays the main region of theoretical and experimental activity in heavy-ion collisions aimed at the study of such VP effects [9,11–14].

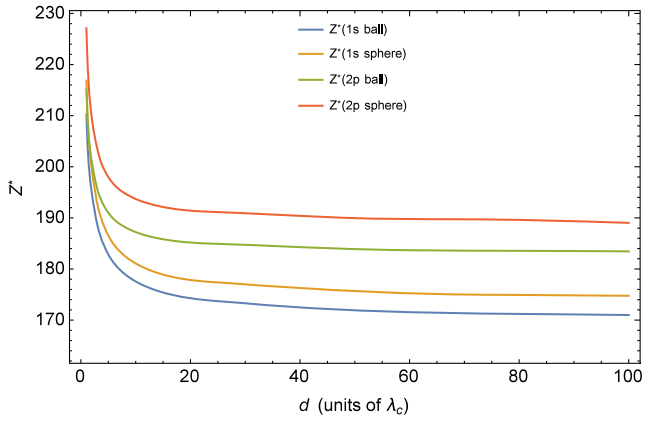

FIG. 8. $Z^*_\pm(d)$ for $1 \le d \le 100$.

It would be worth noting that, if allowed by the lepton number, spontaneous positrons can by no means be emitted also just beyond the corresponding diving point. In particular, for $d = 137$ (one Bohr radius) one obtains $Z^*_{1s}(137) \simeq 174.0, Z^*_{2p}(137) \simeq 188.8$ (sphere) and $Z^*_{1s}(137) \simeq 170.7$, $Z^*_{2p}(137) \simeq 183.3$ (ball), which lie quite close to the corresponding $Z_{{\rm cr},i}$. However, in this case they appear in scattering states localized far enough from the Coulomb source with very small $\epsilon_{\rm kin} \sim 0.01$. Therefore, the creation of such positrons should be strongly suppressed and so cannot significantly alter the nuclear conversion pairs background. To the contrary, vacuum positrons created with $d \simeq 1$ would reveal a high peak, which allows for an unambiguous detection, but the charge of the Coulomb source should be taken in this case to be not less than $Z^* \simeq 210$. The negative result of early investigations at GSI [38] can be at least partially explained by the last circumstance.

VII. CONCLUDING REMARKS

To conclude, it should be mentioned first that, like the one- and two-dimensional models of supercriticality in QED systems [7,8,24,27,29,30,39], in the present case the evaluation of VP energy by means of the renormalization procedure (46)–(48) proceeds similar to, but actually without any references to, VP density and vacuum shells formation. So the renormalization via fermionic loop turns out to be a universal tool, which removes the divergence of the theory both in the purely perturbative and in the essentially nonperturbative regimes of vacuum polarization by the external electromagnetic field. Moreover, such approach can be easily extended to the study of VP effects in more complicated problems, e.g., with two Coulomb centers or including an axial magnetic field, when the spherical symmetry is lost, and so there remains only j_z as a conserved angular quantum number.

The substantial decrease of $\mathcal{E}^{\rm ren}_{\rm VP}(Z)$ in the overcritical region $\sim -Z^4/R$ can be reliably justified via the properties of partial terms in the series (46). Each $\mathcal{E}^{\rm ren}_{{\rm VP},l}(Z)$ in (46) has

the structure, which by omitting the degeneracy factor $2(l+1)$ is quite similar to $\mathcal{E}^{\rm ren}_{\rm VP}(Z)$ in $1+1$ dimensions [7,8]. The direct consequence is that, in the overcritical region, the negative contribution from the renormalization term $\zeta_l Z^2$ turns out to be the dominant one in $\mathcal{E}^{\rm ren}_{{\rm VP},l}(Z)$, since in this region the growth rate of the nonrenormalized partial VP energies (25), as in $1+1$ and $2+1$ dimensions, is estimated as $\sim Z^\nu, 1<\nu<2$. Such estimate is clearly seen in the plots shown in Fig. 4, where both the phase integral and the sum over discrete levels reveal an almost quadratic growth before first level diving, but afterward their curves undergo either bending or negative jumps, which noticeably change the slope of the curves. So, in essence, the decrease of $\mathcal{E}^{\rm ren}_{\rm VP}$ in the overcritical region is governed by the nonperturbative changes in the VP density for $Z > Z_{\rm cr,1}$ due to discrete levels diving into the lower continuum. Furthermore, the total number of partial channels, in which the levels have already sunk into the lower continuum, grows approximately linearly with increasing Z. At the same time, indeed these channels yield the main contribution to VP energy (see Tables I and II). So the rate of decrease of the total VP energy into the negative range acquires an additional factor $\sim Z^2$, which in turn leads to the final answer $\mathcal{E}^{\rm ren}_{\rm VP}(Z) \sim -Z^4/R$ in the overcritical region. Moreover, estimating the self-energy contribution to the radiative part of QED effects due to virtual photon exchange near the lower continuum shows that it is just a perturbative correction to essentially nonlinear VP effects caused by fermionic loop [10], and so does not alter the results presented above.

Lepton number also poses serious questions for both theory and experiment dealing with Coulomb supercriticality, since the emitted positrons must carry away the lepton number equal to $(-1)\times$ their total number. Hence, the corresponding amount of positive lepton numbers must be transferred to VP density, concentrated in vacuum shells. In this case, instead of integer lepton number of real particles, there should appear the lepton number VP density. Otherwise, either the lepton number conservation in such processes must be broken or the positron emission prohibited. So any reliable answer concerning the spontaneous positron emission—either positive or negative—is important for our understanding of the nature of this number, since so far leptons show up as pointlike particles with no indications on existence of any kind intrinsic structure. Therefore, the reasonable conditions, under which the vacuum positron emission can be unambiguously detected on the nuclear conversion pair background, should play an exceptional role in slow ion collisions, aimed at the search of such events [40].

ACKNOWLEDGMENTS

The authors are very indebted to Dr. Yu. S. Voronina, Dr. O. V. Pavlovsky, and A. A. Krasnov from MSU Department of Physics and to Dr. A. S. Davydov from Kurchatov Center for interest and helpful discussions. This work has been supported in part by the Russian Federation Ministry of Science and Education Scientific Research Program, Projects No. 01-2014-63889 and No. A16-116021760047-5, and by RFBR Grant No. 14-02-01261. The research was carried out using the equipment of the shared research facilities of HPC computing resources at Moscow Lomonosov State University.

APPENDIX A: $I(l)$ FOR $l \gg Q$

For these purposes we replace first $\delta_{\rm tot}(l,k)$ by the total WKB phase (31). In the limit (26) the difference between $\delta_{\rm tot}(l,k)$ and $\delta^{\rm WKB}_{\rm tot}(l,k)$ shows up only in oscillations of the exact phase for large k, caused by diffraction on a sphere of the radius R, but they are smoothed upon integration over dk, and so this difference can be freely ignored.

Proceeding further, we rewrite $I(l)$ as

$$I(l) = \frac{1}{\pi}\int_1^\infty d\epsilon\, \delta^{\rm WKB}_{\rm tot}(l,\epsilon) \tag{A1}$$

and introduce in (A1) an intermediate UV cutoff Λ. The latter is necessary to provide permutations in the sequence of integrations. As a result, upon introducing the turning point

$$r_0 = \frac{(l+1)^2 - Q^2}{2Q} \gg R, \tag{A2}$$

and the subsidiary function

$$W(l,r) = \sqrt{1+(l+1)^2/r^2}, \tag{A3}$$

the expression (A1) can be represented as

$$I(l) = \frac{2}{\pi}\lim_{\Lambda\to\infty}\left\{\left[\int_0^{r_0} dr \int_{V(r)+W(l,r)\geq 1}^{\Lambda} d\epsilon + \int_{r_0}^{\infty} dr \int_1^{\Lambda} d\epsilon\right]\sqrt{(\epsilon - V(r))^2 - W^2(l,r)}\right.$$
$$\left. + \int_0^\infty dr \int_{-V(r)+W(l,r)\geq 1}^{\Lambda} d\epsilon \sqrt{(\epsilon+V(r))^2 - W^2(l,r)} - 2\int_0^\infty dr \int_1^\Lambda d\epsilon \sqrt{\epsilon^2 - W^2(l,r)}\right\}, \tag{A4}$$

where the first term originates from $\delta_+(l,k)$, the second one comes from $\delta_-(l,k)$, and the last one comes from $\delta_0(l,k)$. Thereafter, we replace $\epsilon - V(r) \to tW(l,r)$ in the first term, $\epsilon + V(r) \to tW(l,r)$ in the second, and $\epsilon \to tW(l,r)$ in the last one, which gives

$$I(l) = \frac{2}{\pi}\lim_{\Lambda\to\infty}\left\{\left[\int_0^{r_0} dr\, W^2(l,r)\int_1^{\frac{\Lambda-V(r)}{W(l,r)}} dt + \int_{r_0}^{\infty} dr\, W^2(l,r)\int_{\frac{1-V(r)}{W(l,r)}}^{\frac{\Lambda-V(r)}{W(l,r)}} dt\right]\sqrt{t^2-1}\right.$$
$$\left. + \int_0^{\infty} dr\ W^2(l,r)\int_1^{\frac{\Lambda+V(r)}{W(l,r)}} dt\,\sqrt{t^2-1} - 2\int_0^{\infty} dr\ W^2(l,r)\int_1^{\Lambda/W(l,r)} dt\,\sqrt{t^2-1}\right\}. \tag{A5}$$

Introducing further the subsidiary function

$$Y(x) = \frac{1}{2}\left[x\sqrt{x^2-1} - \ln\left(x+\sqrt{x^2-1}\right)\right], \tag{A6}$$

we recast the expression (A5) in the form

$$I(l) = \frac{2}{\pi}\lim_{\Lambda\to\infty}\left\{\int_0^{\infty} dr W^2(l,r)\left[Y\left(\frac{\Lambda+V(r)}{W(l,r)}\right) + Y\left(\frac{\Lambda-V(r)}{W(l,r)}\right) - 2Y\left(\frac{\Lambda}{W(l,r)}\right)\right]\right.$$
$$\left. - \int_{r_0}^{\infty} dr\, W^2(l,r) Y\left(\frac{1-V(r)}{W(l,r)}\right)\right\}. \tag{A7}$$

Since by construction there holds $|V(r)| \ll \Lambda$ for all $0 \le r \le \infty$, we can freely expand the square bracket in (A7) in the power series with the expansion parameter $V(r)/W(l,r)$ in the vicinity of the point $\Lambda/W(l,r)$. Thereafter, by noticing that for $\Lambda \to \infty$ there survives in this expansion only the term with second derivative $Y''(\Lambda) = \Lambda/\sqrt{\Lambda^2-1} \to 1$, one obtains

$$I(l) = I_0 + \Delta I(l), \tag{A8}$$

where

$$I_0 = \frac{2}{\pi}\int_0^{\infty} dr\, V^2(r), \tag{A9}$$

and

$$\Delta I(l) = -\frac{2}{\pi}\int_{r_0}^{\infty} dr\, W^2(l,r) Y\left(\frac{1-V(r)}{W(l,r)}\right). \tag{A10}$$

The most important feature for the present analysis of I_0 is that for any extended Coulomb-like source the integral on the rhs of (A9) converges and is an $O(Q^2)$ quantity. The concrete value of I_0 depends on the profile of the Coulomb source chosen (sphere, ball, or spherical layer), but there is no need to dive into such details here.

The remaining integral (A10) can be easily calculated analytically and so the leading-order WKB answer for $I(l)$ subject to condition (26) reads

$$I(l) = I_0 - 2(l+1-\varkappa_l)$$
$$= \frac{2}{\pi}\int_0^{\infty} dr V^2(r) - \frac{Q^2}{l+1} - \frac{Q^4}{4(l+1)^3} + O\left(\frac{Q^6}{(l+1)^5}\right). \tag{A11}$$

The next-to-leading orders of the WKB approximation for the total phase lead to $O(Q^4/(l+1)^3)$ corrections [25]. Hence, the large l asymptotics of the partial phase integral reads

$$I(l) \to \frac{2}{\pi}\int_0^{\infty} dr\, V^2(r) - \frac{Q^2}{l+1} + O\left(\frac{Q^4}{(l+1)^3}\right), \quad l \to \infty. \tag{A12}$$

APPENDIX B: SLICING THE BALL CONFIGURATION

The simplest grid for such approximation of $V(r)$ inside the ball, that means for $0 \le r \le R$, can be chosen in the form

$$R_i = \sqrt{\frac{i}{N}}R, \qquad V_i = -\frac{3Q}{2R} + \frac{i}{2N}\frac{Q}{R}, \tag{B1}$$

where $1 \le i \le N$ is the numerator of separate segments with constant values of the potential V_i. Note that the grid is uniform in the step between subsequent V_i,

$$\Delta V = V_i - V_{i-1} = \frac{1}{2N}\frac{Q}{R}, \tag{B2}$$

but not uniform in the length of subsequent segments in the radial variable. This is made specially to optimize the approximation of parabolic behavior of $V(r)$ on this interval. Within such a grid, the solution of the DC problem for the ball case proceeds as follows. As in the case of the sphere, we start with assembling the total phase $\delta_{\rm tot}(l,k)$ from (u_l, q_l) and (p_l, v_l) components using the crossing symmetry to restore the contribution from the (p_l, v_l) pair via the (u_l, q_l) pair. For the latter, in the upper continuum with $\epsilon(k) = \sqrt{k^2+1} \ge 1$ upon introducing

$$\xi_i(k) = \sqrt{(\epsilon(k) - V_i)^2 - 1}, \tag{B3}$$

the corresponding solutions on the ith radial segment $(i = 1, \ldots, N)$ with $R_{i-1} \le r \le R_i$ should be written as

$$\begin{cases} u_l(k,r) = \sqrt{\epsilon(k) - V_i + 1}[J_{l+1/2}(\xi_i(k)r) + \sigma_i(l,k)Y_{l+1/2}(\xi_i(k)r)]/\sqrt{r}, \\ q_l(k,r) = -\sqrt{\epsilon(k) - V_i - 1}[J_{l+3/2}(\xi_i(k)r) + \sigma_i(l,k)Y_{l+3/2}(\xi_i(k)r)]/\sqrt{r}, \end{cases} \tag{B4}$$

with $Y_\nu(z)$ being the Neumann function.

The coefficients σ_i in Eqs. (B4) are determined from the following recurrence relations:

$$\sigma_1(l,k) = 0, \tag{B5}$$

$$\sigma_i(l,k) = -U_1(i)/U_2(i), \quad 2 \le i \le N, \tag{B6}$$

where

$$\begin{cases} U_1(i) = \sqrt{\epsilon(k) - V_{i-1} + 1}\sqrt{\epsilon(k) - V_i - 1}[J_{l+1/2}(\xi_{i-1}(k)R_{i-1}) + \sigma_{i-1}(l,k)Y_{l+1/2}(\xi_{i-1}(k)R_{i-1})]J_{l+3/2}(\xi_i(k)R_{i-1}) \\ -\sqrt{\epsilon(k) - V_{i-1} - 1}\sqrt{\epsilon(k) - V_i + 1}[J_{l+1/2}(\xi_{i-1}(k)R_{i-1}) + \sigma_{i-1}(l,k)Y_{l+1/2}(\xi_{i-1}(k)R_{i-1})]J_{l+1/2}(\xi_i(k)R_{i-1}), \\ U_2(i) = \sqrt{\epsilon(k) - V_{i-1} + 1}\sqrt{\epsilon(k) - V_i - 1}[J_{l+1/2}(\xi_{i-1}(k)R_{i-1}) + \sigma_{i-1}(l,k)Y_{l+1/2}(\xi_{i-1}(k)R_{i-1})]Y_{l+3/2}(\xi_i(k)R_{i-1}) \\ -\sqrt{\epsilon(k) - V_{i-1} - 1}\sqrt{\epsilon(k) - V_i + 1}[J_{l+1/2}(\xi_{i-1}(k)R_{i-1}) + \sigma_{i-1}(l,k)Y_{l+1/2}(\xi_{i-1}(k)R_{i-1})]Y_{l+1/2}(\xi_i(k)R_{i-1}). \end{cases} \tag{B7}$$

Upon solving the recurrences (B5)–(B7), one finds the set of coefficients σ_i and so the solutions for the (u_l, q_l) pair in each segment $R_{i-1} \le r \le R_i$ of the grid, which are sewn together by continuity at points R_i. As a result, for the matching point $R = R(Z)$ between inner and outer solutions of the DC problem, one obtains from the inside

$$\begin{cases} u_l(k,R) = \sqrt{\epsilon(k) + V_0 + 1}[J_{l+1/2}(\xi R) + \sigma_N(l,k)Y_{l+1/2}(\xi R)]/\sqrt{R}, \\ q_l(k,R) = -\sqrt{\epsilon(k) + V_0 - 1}[J_{l+3/2}(\xi R) + \sigma_N(l,k)Y_{l+3/2}(\xi R)]/\sqrt{R}, \end{cases} \tag{B8}$$

where as in Sec. IV $\xi = \xi(k) = \sqrt{(\epsilon(k) + V_0)^2 - 1}, V_0 = Q/R$.

At the same time, the outer solutions remain the same as for the sphere. Therefore, by means of the expression (B8), stitching the inner and outer solutions of the DC problem for the charged ball in the upper continuum proceeds very simply by means of the following replacement in the matching coefficients $\lambda^+_{uq}(l,k)$ and $N_R(l,k)$, defined in (58) and (75) for the case of the charged sphere:

$$\begin{cases} J_{l+1/2}(\xi R) \to J_{l+1/2}(\xi R) + \sigma_N(l,k) Y_{l+1/2}(\xi R), \\ J_{l+3/2}(\xi R) \to J_{l+3/2}(\xi R) + \sigma_N(l,k) Y_{l+3/2}(\xi R). \end{cases} \tag{B9}$$

Thereafter, the phase shifts $\delta^{+}_{uq}(l,k)$ for the ball are obtained from those of the sphere via replacing the matching coefficients $\lambda^{+}_{uq}(l,k)$ and $N_R(l,k)$ by the new ones, determined by the substitutions (B9).

In the lower continuum with $\epsilon(k) = -\sqrt{k^2+1} < -1$ for each segment $R_{i-1} \le r \le R_i$ of the grid, the half-axis $0 \le k \le \infty$ should be again divided in three intervals $0 \le k \le k_1(i), k_1(i) \le k \le k_2(i)$ and $k_2(i) \le k \le \infty$, where

$$k_1(i) = \sqrt{(1+V_i)^2 - 1} < k_2(i) = \sqrt{(1-V_i)^2 - 1}, \quad 1 \le i \le N, \tag{B10}$$

while $k_1(N)$ and $k_2(N)$ coincide with k_1 and k_2, defined earlier in Eq. (63). Upon introducing

$$\tilde{\xi}_i(k) = \sqrt{1 - (\epsilon(k) - V_i)^2}, \tag{B11}$$

the solutions for the ith segment $R_{i-1} \le r \le R_i$ in this case are written as follows:

$$u_l(k,r) = \sqrt{||\epsilon(k)| + V_i - 1|} \begin{cases} J_{l+1/2}(\xi_i(k)r) + \sigma_{i1}(l,k) Y_{l+1/2}(\xi_i(k)r), & 0 \le k \le k_1(i), \\ I_{l+1/2}(\tilde{\xi}_i(k)r) + \sigma_{i2}(l,k)) K_{l+1/2}(\tilde{\xi}_i(k)r), & k_1(i) \le k \le k_2(i), \\ J_{l+1/2}(\xi_i(k)r) + \sigma_{i3}(l,k) Y_{l+1/2}(\xi_i(k)r), & k_2(i) \le k \le \infty, \end{cases} \tag{B12}$$

$$q_l(k,r) = \sqrt{||\epsilon(k)| + V_i + 1|} \begin{cases} -(J_{l+3/2}(\xi_i(k)r) + \sigma_{i1}(l,k) Y_{l+3/2}(\xi_i(k)r)), & 0 \le k \le k_1(i), \\ I_{l+3/2}(\tilde{\xi}_i(k)r) - \sigma_{i2}(l,k) K_{l+3/2}(\tilde{\xi}_i(k)r), & k_1(i) \le k \le k_2(i), \\ J_{l+3/2}(\xi_i(k)r) + \sigma_{i3}(l,k) Y_{l+3/2}(\xi_i(k)r), & k_2(i) \le k \le \infty. \end{cases} \tag{B13}$$

Stitching the solutions (B12) and (B13) separately at points $R_i, i = 1, \ldots, N-1$, one obtains the recurrence relations for the coefficients $\sigma_{ij}(l,k), j = 1, 2, 3$, which are solved with initial conditions

$$\sigma_{1j}(l,k) = 0, \quad j = 1,2,3. \tag{B14}$$

Afterward, the phase shifts $\delta^{-}_{uq}(l,k)$ for the ball are obtained from those for the sphere by the same procedure of replacing the matching coefficients $\lambda^{-}_{uq}(l,k)$ and $N_R(l,k)$ by the new ones, determined through the set of substitutions, similar to (B9). The main difference is that this procedure should be now implemented separately for each of three intervals $0 \le k \le k_1(N), k_1(N) \le k \le k_2(N)$, and $k_2(N) \le k \le \infty$.

The discrete spectrum for the charged ball configuration is found from the corresponding equations for the sphere (92) and (93) with the replacement (B9), where instead of $\epsilon(k) = \sqrt{k^2+1} \ge 1$ in all the expressions, including the recurrences (B5)–(B7), one should insert ϵ, which is subject to condition $|\epsilon| < 1$. Proceeding further this way, for the levels with $\epsilon = -1$ and so for the corresponding critical charges one obtains the equations similar to Eqs. (96) and (97), where instead of $J_{\pm}$ defined in (97) one should insert now the combinations

$$J_{\pm} + \gamma_N(l) Y_{\pm}, \tag{B15}$$

where

$$Y_{-} = Y_{l+1/2}(z_1), \qquad Y_{+} = Y_{l+3/2}(z_1), \tag{B16}$$

z_1 is defined in (97), while $\gamma_N(l)$ are found from the recurrences (B5)–(B7) with the replacement $\epsilon(k) \to -1$.

Applying such procedure to the search for critical charges in the ball configuration, one finds for the grid with $N = 1000$ segments the results, which coincide with those obtained via direct numerical solution of DE in all the characters given below. In particular, with the same relation (101) for $R(Z)$ for the lowest $1s_{1/2}$ and $2p_{1/2}$ levels, one finds $Z_{\mathrm{cr},1} \simeq 170.0048$ and $Z_{\mathrm{cr},2} \simeq 183.0756$, correspondingly. Compared to the case of the sphere with $Z_{\mathrm{cr},1} \simeq 173.613$ and $Z_{\mathrm{cr},2} \simeq 188.5497$, in the ball case the diving points reveal a small shift to the left. Actually, the last circumstance is a common feature of all the dived levels in the ball case, but with each subsequent diving point it becomes less and less pronounced.

[1] J. Rafelski, J. Kirsch, B. Müller, J. Reinhardt, and W. Greiner, Probing QED vacuum with heavy ions, in *New Horizons in Fundamental Physics*, FIAS Interdisciplinary Science Series (Springer, New York, 2017), pp. 211–251.

[2] W. Greiner, B. Müller, and J. Rafelski, *Quantum Electrodynamics of Strong Fields*, 2nd ed. (Springer, Berlin, 1985).

[3] G. Plunien, B. Müller, and W. Greiner, The Casimir effect, Phys. Rep. **134**, 87 (1986).

[4] W. Greiner and J. Reinhardt, *Quantum Electrodynamics*, 4th ed. (Springer-Verlag, Berlin, Heidelberg, 2009).

[5] R. Ruffini, G. Vereshchagin, and S.-S. Xue, Electron–positron pairs in physics and astrophysics: From heavy nuclei to black holes, Phys. Rep. **487**, 1 (2010).

[6] V. M. Kuleshov, V. D. Mur, N. B. Narozhny, A. M. Fedotov, and Y. E. Lozovik, Coulomb problem for graphene with the gapped electron spectrum, JETP Lett. **101**, 264 (2015); V. M. Kuleshov, V. D. Mur, N. B. Narozhny, A. M. Fedotov, Y. E. Lozovik, and V. S. Popov, Coulomb problem for a $Z > Z_{\rm cr}$ nucleus, Phys. Usp. **58**, 785 (2015); S. I. Godunov, B. Machet, and M. I. Vysotsky, Resonances in positron scattering on a supercritical nucleus and spontaneous production of e^+e^- pairs, Eur. Phys. J. C **77**, 782 (2017).

[7] A. Davydov, K. Sveshnikov, and Y. Voronina, Vacuum energy of one-dimensional supercritical Dirac–Coulomb system, Int. J. Mod. Phys. A **32**, 1750054 (2017); Y. Voronina, A. Davydov, and K. Sveshnikov, Nonperturbative effects of vacuum polarization for a quasi-one-dimensional Dirac–Coulomb system with $Z > Z_{cr}$, Phys. Part. Nucl. Lett. **14**, 698 (2017).

[8] Y. Voronina, A. Davydov, and K. Sveshnikov, Vacuum effects for a one-dimensional "hydrogen atom" with $Z > Z_{\rm cr}$, Theor. Math. Phys. **193**, 1647 (2017).

[9] R. Popov, A. Bondarev, Y. Kozhedub, I. Maltsev, V. Shabaev, I. Tupitsyn, X. Ma, G. Plunien, and T. Stöhlker, One-center calculations of the electron-positron pair creation in low-energy collisions of heavy bare nuclei, Eur. Phys. J. D **72**, 115 (2018); O. Novak, R. Kholodov, A. Surzhykov, A. N. Artemyev, and T. Stöhlker, K-shell ionization of heavy hydrogenlike ions, Phys. Rev. A **97**, 032518 (2018); I. A. Maltsev, V. M. Shabaev, R. V. Popov, Y. S. Kozhedub, G. Plunien, X. Ma, and T. Stöhlker, Electron-positron pair production in slow collisions of heavy nuclei beyond the monopole approximation, Phys. Rev. A **98**, 062709 (2018).

[10] A. Roenko and K. Sveshnikov, Estimating the radiative part of QED effects in superheavy nuclear quasimolecules, Phys. Rev. A **97**, 012113 (2018).

[11] I. A. Maltsev, V. M. Shabaev, R. V. Popov, Y. S. Kozhedub, G. Plunien, X. Ma, T. Stöhlker, and D. A. Tumakov, How to Observe the Vacuum Decay in Low-Energy Heavy-Ion Collisions, Phys. Rev. Lett. **123**, 113401 (2019); R. V. Popov, V. M. Shabaev, D. A. Telnov, I. I. Tupitsyn, I. A. Maltsev, Y. S. Kozhedub, A. I. Bondarev, N. V. Kozin, X. Ma, G. Plunien, T. Stöhlker, D. A. Tumakov, and V. A. Zaytsev, How to access QED at a supercritical Coulomb field, Phys. Rev. D **102**, 076005 (2020).

[12] A. Gumberidze, T. Stöhlker, H. F. Beyer, F. Bosch, A. Bräuning-Demian, S. Hagmann, C. Kozhuharov, T. Kühl, R. Mann, P. Indelicato, W. Quint, R. Schuch, and A. Warczak, X-ray spectroscopy of highly-charged heavy ions at FAIR, Nucl. Instrum. Methods Phys. Res., Sect. B **267**, 248 (2009).

[13] G. M. Ter-Akopian, W. Greiner, I. Meshkov, Y. Oganessian, J. Reinhardt, and G. Trubnikov, Layout of new experiments on the observation of spontaneous electron–positron pair creation in supercritical Coulomb fields, Int. J. Mod. Phys. E **24**, 1550016 (2015).

[14] X. Ma, W. Wen, S. Zhang, D. Yu, R. Cheng, J. Yang, Z. Huang, H. Wang, X. Zhu, X. Cai, Y. Zhao, L. Mao, J. Yang, X. Zhou, H. Xu, Y. Yuan, J. Xia, H. Zhao, G. Xiao, and W. Zhan, HIAF: New opportunities for atomic physics with highly charged heavy ions, Nucl. Instrum. Methods Phys. Res., Sect. B **408**, 169 (2017).

[15] E. H. Wichmann and N. M. Kroll, Vacuum polarization in a strong Coulomb field, Phys. Rev. **101**, 843 (1956).

[16] M. Gyulassy, Higher order vacuum polarization for finite radius nuclei, Nucl. Phys. **A244**, 497 (1975).

[17] L. Brown, R. Cahn, and L. McLerran, Vacuum polarization in a strong Coulomb field. I. Induced point charge, Phys. Rev. D **12**, 581 (1975); Vacuum polarization in a strong Coulomb field. II. Short-distance corrections, **12**, 596 (1975); Vacuum polarization in a strong Coulomb field. III. Nuclear size effects, **12**, 609 (1975).

[18] J. Schwinger, Quantum electrodynamics. II. Vacuum polarization and self-energy, Phys. Rev. **75**, 651 (1949); On gauge invariance and vacuum polarization, **82**, 664 (1951).

[19] C. Itzykson and J.-B. Zuber, *Quantum Field Theory* (McGraw-Hill, New York, 1980).

[20] R. Rajaraman, *Solitons and Instantons*, 1st ed. (North-Holland Publishing Company, Amsterdam, 1982).

[21] K. Sveshnikov, Dirac sea correction to the topological soliton mass, Phys. Lett. B **255**, 255 (1991).

[22] P. Sundberg and R. L. Jaffe, The Casimir effect for fermions in one dimension, Ann. Phys. (Amsterdam) **309**, 442 (2004).

[23] A. Chodos, R. L. Jaffe, K. Johnson, C. B. Thorn, and V. F. Weisskopf, New extended model of hadrons, Phys. Rev. D **9**, 3471 (1974).

[24] A. Davydov, K. Sveshnikov, and Y. Voronina, Nonperturbative vacuum polarization effects in twodimensional supercritical Dirac–Coulomb system II. Vacuum energy, Int. J. Mod. Phys. A **33**, 1850005 (2018).

[25] V. Lazur, O. Reity, and V. Rubish, WKB method for the Dirac equation with a scalar-vector coupling, Theor. Math. Phys. **143**, 559 (2005); B. Zon and A. Kornev, Semiclassical approximation of the Dirac equation in a central field, Theor. Math. Phys. **171**, 478 (2012).

[26] Y. Voronina, I. Komissarov, and K. Sveshnikov, Casimir interactions between two short-range Coulomb sources, Ann. Phys. (Amsterdam) **404**, 132 (2019); Casimir force variability in one-dimensional QED systems, Phys. Rev. A **99**, 062504 (2019).

[27] P. Grashin and K. Sveshnikov, Magnetic vacuum polarization effects in the supercritical QED: Spontaneous generation of the ferromagnetic vacuum state above the "Curie point" $Z \geq Z^* > Z_{cr}$, Ann. Phys. (Amsterdam) **415**, 168094 (2020); Ferromagnetic phase in graphene-based planar heterostructures induced by charged impurity, Ann. Phys. (Berlin) **415**, 351 (2020).

[28] V. Berestetskii, L. Pitaevskii, and E. Lifshitz, *Quantum Electrodynamics* (Elsevier, New York, 2012), Vol. 4.

[29] A. Davydov, K. Sveshnikov, and Y. Voronina, Nonperturbative vacuum polarization effects in twodimensional supercritical Dirac–Coulomb system I. Vacuum charge density, Int. J. Mod. Phys. A **33**, 1850004 (2018).

[30] K. Sveshnikov, Y. Voronina, A. Davydov, and P. Grashin, Essentially nonperturbative vacuum polarization effects in a two-dimensional Dirac–Coulomb system with $Z > Z_{cr}$: Vacuum charge density, Theor. Math. Phys. **198**, 331 (2019); Essentially nonperturbative vacuum polarization effects in a two-dimensional Dirac–Coulomb system for $Z > Z_{cr}$: Vacuum polarization effects, **199**, 533 (2019).

[31] P. J. Mohr, G. Plunien, and G. Soff, QED corrections in heavy atoms, Phys. Rep. **293**, 227 (1998).

[32] H. Bateman and A. Erdelyi, *Higher Transcendental Functions* (McGraw-Hill, New York, 1953), Vol. 1–2.

[33] Y. B. Zeldovich and V. S. Popov, Electronic structure of superheavy atoms, Sov. Phys. Usp. **14**, 673 (1972).

[34] U. Fano, Effects of configuration interaction on intensities and phase shifts, Phys. Rev. **124**, 1866 (1961).

[35] J. Reinhardt, B. Müller, and W. Greiner, Theory of positron production in heavy-ion collisions, Phys. Rev. A **24**, 103 (1981); U. Müller, T. de Reus, J. Reinhardt, B. Müller, W. Greiner, and G. Soff, Positron production in crossed beams of bare uranium nuclei, Phys. Rev. A **37**, 1449 (1988).

[36] E. Ackad and M. Horbatsch, Calculation of electron-positron production in supercritical uranium-uranium collisions near the Coulomb barrier, Phys. Rev. A **78**, 062711 (2008).

[37] A. Marsman and M. Horbatsch, Calculation of supercritical Dirac resonance parameters for heavy-ion systems from a coupled-differential-equation approach, Phys. Rev. A **84**, 032517 (2011); I. Maltsev, V. Shabaev, V. Zaytsev, R. V. Popov, Y. S. Kozhedub, and D. A. Tumakov, Calculation of the energy and width of supercritical resonance in a uranium quasimolecule, Opt. Spectrosc. **128**, 1100 (2020).

[38] U. Müller-Nehler and G. Soff, Electron excitations in superheavy quasimolecules, Phys. Rep. **246**, 101 (1994).

[39] Y. Voronina, K. Sveshnikov, P. Grashin, and A. Davydov, Essentially non-perturbative and peculiar polarization effects in planar QED with strong coupling, Physica (Amsterdam) **106E**, 298 (2019); Casimir (vacuum) energy in planar QED with strong coupling, **109**, 209 (2019).

[40] A. Krasnov and K. Sveshnikov, Lepton number vs Coulomb super-criticality, arXiv:2201.04829.